Position-specific kinetic isotope effects for nitrous oxide: A new expansion of the Rayleigh model

Elise D. Rivett[1,2,*], Wenjuan Ma[3], Nathaniel E. Ostrom[2,4,*], Eric L. Hegg[1,2,*]

[1] Department of Biochemistry & Molecular Biology, Michigan State University, East Lansing, Michigan 48824, United States
5 [2] DOE Great Lakes Bioenergy Research Center, Michigan State University, East Lansing, MI, 48824, United States
[3] Center for Statistical Training and Consulting, Michigan State University, East Lansing, MI, 48824, United States
[4] Department of Integrative Biology, Michigan State University, East Lansing, Michigan 48824, United States

Correspondence to: Elise D. Rivett (rivettel@msu.edu), Nathaniel E. Ostrom (ostromn@msu.edu), Eric L. Hegg (erichegg@msu.edu)

10 **Abstract.** Nitrous oxide (N_2O) is a potent greenhouse gas and the most significant anthropogenic ozone-depleting substance currently being emitted. A major source of anthropogenic N_2O emissions is the microbial conversion of fixed nitrogen species from fertilizers in agricultural soils. Thus, understanding the enzymatic mechanisms by which microbes produce N_2O has environmental significance. Measurement of the $^{15}N/^{14}N$ isotope ratios of N_2O produced by purified enzymes or axenic microbial cultures is a promising technique for studying N_2O biosynthesis. Typically, N_2O-producing enzymes combine
15 nitrogen atoms from two identical substrate molecules (NO or NH_2OH). Position-specific isotope analysis of the central (N^α) and outer (N^β) nitrogen atoms in N_2O enables the determination of the individual kinetic isotope effects (KIEs) for N^α and N^β, providing mechanistic insight into the incorporation of each nitrogen atom. Previously, position-specific KIEs (and fractionation factors) were quantified using the Rayleigh distillation equation, *i.e.*, via linear regression of $\delta^{15}N^\alpha$ or $\delta^{15}N^\beta$ against [-flnf/(1-f)], where f is the fraction of substrate remaining in a closed system. This approach, however, is inaccurate
20 for N^α and N^β because it does not account for fractionation at N^α affecting the isotopic composition of substrate available for incorporation into the β position (and vice versa). Therefore, we developed a new expansion of the Rayleigh model that includes specific terms for fractionation at the individual N_2O nitrogen atoms. By applying this Expanded Rayleigh model to a variety of simulated N_2O synthesis reactions with different combinations of normal/inverse/no KIEs at N^α and N^β, we demonstrate that our new model is both accurate and robust. We also applied this new model to two previously published
25 datasets describing N_2O production from NH_2OH oxidation in a methanotroph culture (*Methylosinus trichosporium*) and N_2O production from NO by a purified *Histoplasma capsulatum* (fungal) P450 NOR, demonstrating that the Expanded Rayleigh model is a useful tool in calculating position-specific fractionation for N_2O synthesis.

1 Introduction

Nitrous oxide (N_2O) is a greenhouse gas with a global warming potential approximately 300 times greater than that of CO_2
30 (100-year time horizon) Stocker (2013). In addition, N_2O is the primary source of stratospheric NO_x and therefore is a

significant ozone-depleting substance (Ravishankara et al., 2009). Levels of atmospheric N_2O are increasing by an average of ~0.29% annually (Lan et al., 2022), primarily due to rising anthropogenic N_2O emissions, which comprise approximately 40% of annual global N_2O emissions (Tian et al., 2020). In the US, at least 70% of annual anthropogenic N_2O emissions result from agricultural practices, such as the application of nitrogen-containing fertilizer (*e.g.*, ammonium and nitrate) to the field. Soil

35   microbes can metabolize these nitrogen-containing compounds through processes such as nitrification and denitrification, producing N_2O either as a side-product (nitrification), intermediate (complete denitrification), or end-product (incomplete denitrification) (Kuypers et al., 2018). Understanding the underlying mechanisms of N_2O production for each metabolic pathway is critical for tracing and ultimately mitigating environmental N_2O emissions.

Many different types of enzymes catalyze N_2O formation in microbes. Examples of N_2O-producing enzyme families

40   include cytochrome P460 (Caranto et al., 2016) and hydroxylamine oxidoreductase (Yamazaki et al., 2014) in nitrifiers, "bacterial" nitric oxide reductases (cNOR, qNOR, etc.) found in bacterial/archaeal denitrifiers, and fungal nitric oxide reductase (P450 NOR) from fungal denitrifiers (Yamazaki et al., 2014; Yang et al., 2014; Lehnert et al., 2018) as well as detoxifying enzymes such as flavodiiron nitric oxide reductases (Romão et al., 2016). Distinguishing among different sources of N_2O in the environment and identifying the relative contribution of each source is challenging and requires a combination

45   of analytical methods. One useful technique for N_2O source apportionment is compound-specific stable isotope analysis, or the measurement of isotope ratios in a particular chemical compound. This method takes advantage of the fact that many physical and chemical processes, such as enzyme-catalyzed reactions, generally have slightly different rate constants for different isotopes of the same element (*e.g.*, ^{14}N and ^{15}N). In an isotopically sensitive process, the isotope that reacts faster will be more prevalent (enriched) in the product relative to the substrate. Different processes generally have distinct patterns

50   of isotopic enrichment and thus have unique isotopic signatures.

Stable isotope analysis is particularly useful for studying N_2O synthesis because the central (N^{α}) and outer (N^{β}) nitrogen atoms in N_2O are non-equivalent and non-exchangeable, and the isotope ratios of these two nitrogen atoms can be determined individually (Toyoda and Yoshida, 1999). These position-specific isotope ratios can aid in identifying which enzyme(s) produce N_2O in microbial cultures under varying growth conditions (Sutka et al., 2003, 2004; Sutka et al., 2006;

55   Sutka et al., 2008; Toyoda et al., 2005; Frame and Casciotti, 2010; Yamazaki et al., 2014; Haslun et al., 2018). Additionally, because isotopic enrichment is typically dependent on the rate-limiting step(s) of the enzyme-catalyzed reaction, analyzing the isotopic signatures of individual enzymes can provide valuable insights into each enzyme's catalytic mechanism.

Isotopic enrichment for a specific process can be quantified by determining a parameter known as the fractionation factor ($\alpha_{p/s}$). For reactions with first-order kinetics, $\alpha_{p/s}$ is equal to the rate constant of the heavy isotope (k_H) divided by the

60   rate constant for the light isotope (k_L) (Bigeleisen and Wolfsberg, 1958). Because $\alpha_{p/s}$ values are typically close to 1, $\alpha_{p/s}$ is often converted to its per mil equivalent, the enrichment factor ($\varepsilon_{p/s}$):

$$\varepsilon_{p/s} = (\alpha_{p/s} - 1) * 1000 \qquad (1)$$

Notably, $\alpha_{p/s}$ is also equal to the inverse of the kinetic isotope effect (KIE = k_L/k_H). The KIE and fractionation factor values for a specific reaction describe the isotopic preference of that reaction. Most commonly, the light isotope reacts faster than the

65 heavy isotope (*i.e.*, KIE > 1), which is designated as a normal KIE. Conversely, when the heavy isotope reacts faster (KIE < 1), the reaction is said to have an inverse KIE. If the heavy and light isotopes react at the same rate (KIE = 1), the reaction has no kinetic isotope effect.

Mariotti and colleagues (1981) derived an approximation of the Rayleigh distillation equation (hereafter referred to as the (standard) Rayleigh equation) that is frequently used to determine enrichment factors in closed systems (Eq. (2))

70 (Mariotti et al., 1981).

$$\delta^{15}N^p = \delta^{15}N^{s0} - \varepsilon_{p/s} * \frac{fln(f)}{1-f} \tag{2}$$

Here, $\delta^{15}N^p$ is the δ value of accumulated product (p) at time *t*, $\delta^{15}N^{s0}$ is the δ value of the substrate at *t* = 0, and f is the fraction of substrate remaining at time *t* (f = N^s/N^{s0}). (The δ values are directly related to isotope ratios; see "Isotope nomenclature" below.) Notably, the Rayleigh equation is based on the assumption that the element of interest is transferred from the substrate

75 to a single position (or equivalent positions) in the product.

The Rayleigh equation (Eq. (2)) holds true for $\delta^{15}N^{bulk}$ (the average of $\delta^{15}N^{\alpha}$ and $\delta^{15}N^{\beta}$) because the overall reaction can be thought of as the unidirectional conversion of two identical substrate molecules (*e.g.*, two NO or two NH_2OH molecules) to one product molecule with two nitrogen atoms (2S→P$_2$). In the absence of side reactions, this means that $\delta^{15}N^{bulk}$ can be calculated at any point during the reaction (*i.e.*, for any value of f) as long as the δ value of the initial substrate ($\delta^{15}N^{s0}$)

80 and the enrichment factor (ε_{N-bulk}) are known. In practice, the ε_{N-bulk} value for a specific enzymatic reaction is found by plotting $\delta^{15}N^{bulk}$ versus [-flnf/(1-f)][[-flnf/(1-f)]]. Because it is assumed that changes in $\delta^{15}N^{bulk}$ are due solely to the bulk kinetic isotope effect of the reaction in question, the slope of this plot (determined by linear regression) is the bulk enrichment factor (ε_{N-bulk}), and the y-intercept corresponds to $\delta^{15}N^{s0}$.

Unfortunately, the relationship between $\delta^{15}N^{\alpha}$, $\delta^{15}N^{\beta}$, and their corresponding enrichment factors is more complex

85 because the two N atoms are non-exchangeable and both steps that incorporate NO (or NH_2OH) are potentially isotopically sensitive. *In other words, fractionation at the α position alters the isotopic ratio of the remaining substrate ($\delta^{15}N^s$) that is available for incorporation into the β position, and vice versa.* Thus, simply determining the change in $\delta^{15}N^{\alpha}$ (or $\delta^{15}N^{\beta}$) as a function of [-flnf/(1-f)] over the course of the reaction (*i.e.*, finding the slope of a Rayleigh plot via linear regression of $\delta^{15}N^{\alpha}$ or $\delta^{15}N^{\beta}$ against [-flnf/(1-f)]) is not an accurate method for calculating the enrichment factor for N^{α} (or N^{β}).

90 The complexity of calculating enrichment factors for a branched N_2O biosynthesis reaction can be demonstrated mathematically by substituting ½($\delta^{15}N^{\alpha}$ + $\delta^{15}N^{\beta}$) for $\delta^{15}N^p$ and ½($\varepsilon_{N-\alpha}$ + $\varepsilon_{N-\beta}$) for $\varepsilon_{p/s}$ in the Rayleigh equation (Eq. (2)), yielding equation 3:

$$\frac{1}{2}(\delta^{15}N^{\alpha} + \delta^{15}N^{\beta}) = \delta^{15}N^{s0} - \frac{1}{2}(\varepsilon_{N-\alpha} + \varepsilon_{N-\beta})\frac{fln(f)}{1-f} \tag{3}$$

Here, $\varepsilon_{N-\alpha}$ and $\varepsilon_{N-\beta}$ stand for the isotopic enrichment factors for the α and β nitrogen atoms, respectively. Equation 3 can then

95   be rearranged to solve for $\delta^{15}N^\alpha$ (Eq. (4)):

$$\delta^{15}N^\alpha = 2\delta^{15}N^{s0} + \varepsilon_{N-\alpha}\left(-\frac{f\ln(f)}{1-f}\right) + \varepsilon_{N-\beta}\left(-\frac{f\ln(f)}{1-f}\right) - \delta^{15}N^\beta \tag{4}$$

The underlying difficulty in using Eq. (4) is that for a given value of f, $\delta^{15}N^\alpha$ depends not only on $\delta^{15}N^{s0}$ and $\varepsilon_{N-\alpha}$, but also on

$\varepsilon_{N-\beta}$ and the current $\delta^{15}N^\beta$ value. Put another way, we have one equation and two unknowns ($\varepsilon_{N-\alpha}$ and $\varepsilon_{N-\beta}$).

To address this issue, we developed an expanded version of the Rayleigh model that includes specific terms for the

100   individual nitrogen atoms in N_2O. To test the robustness of this new Expanded Rayleigh model, we generated simulated

isotopic data for each of five different potential catalytic mechanisms for N_2O formation. For each N_2O synthesis scenario,

the size and skewness of the simulated measurement error was varied, and 1000 simulated datasets were generated for each

combination of error level and skewness type. We then applied the standard Rayleigh model and Expanded Rayleigh model

to each dataset to determine ε_{N-bulk}, $\varepsilon_{N-\alpha}$, and $\varepsilon_{N-\beta}$ and compared the precision and accuracy of the two models. Finally, we

105   compared the results of applying the standard Rayleigh model and Expanded Rayleigh model to previously published isotopic

data.

2 Methods

2.1 Isotope nomenclature

The isotopic ratio, R, is defined as the abundance of the heavy isotope (^{15}N) divided by the abundance of the light isotope

110   (^{14}N):

$$R = \frac{\text{Heavy Isotope}}{\text{Light Isotope}} = \left(\text{e.g.} \quad \frac{^{15}N}{^{14}N}\right) \tag{5}$$

In the case of nitrogen, ^{14}N is naturally much more abundant than ^{15}N. (Atom percent of ^{15}N in atmospheric N_2 (air) is 0.3663

$\pm$ 0.0004%, so R $\approx$ 0.003663) (Junk and Svec, 1958; Mariotti et al., 1981). The R value of a sample is usually measured relative

to that of a standard ($R_{sample}/R_{standard}$). For nitrogen, the standard is atmospheric N_2. Because there is naturally little variation

115   in ^{15}N, $R_{sample}/R_{standard}$ values are typically close to 1, and isotopic ratios are usually converted to the per mil equivalent, δ,

$$\delta = \left(\left(\frac{R_{sample}}{R_{standard}}\right) - 1\right) * 1000 \tag{6}$$

where R_{sample} is the isotopic ratio of the sample, and $R_{standard}$ is the isotopic ratio of the analytical standard (Mariotti et al.,

1981).

Throughout this manuscript, N^{bulk} is defined as the total number of "equivalents" of nitrogen atoms in N_2O, or 2*(mol

120   of N_2O). N^α and N^β are defined as the number (or moles) of N at the α (central) and β (outer) positions of N_2O, respectively.

$$0.5 * N^{bulk} = N^\alpha = N^\beta = mol\ N_2O \tag{7}$$

Thus, $^{15}N^{bulk}$ is defined as the total number of ^{15}N atoms at both the α and β positions:

$$^{15}N^{bulk} = {}^{15}N^{\alpha} + {}^{15}N^{\beta} \tag{8}$$

Similarly, $^{14}N^{bulk}$ is defined as the total number of ^{14}N at the α and β positions of N_2O:

$$^{14}N^{bulk} = {}^{14}N^{\alpha} + {}^{14}N^{\beta} \tag{9}$$

2.2 α, ε, and KIE

As discussed above, the isotopic fractionation factor ($\alpha_{p/s}$) is equal to the inverse of the kinetic isotope effect (KIE) for first-order reactions and for higher-order reactions when the rare (heavy) isotope is dilute (*i.e.*, ^{15}N or ^{13}C at natural abundance) (Eq. (10)) (Bigeleisen and Wolfsberg, 1958). KIE is defined as the rate constant of the light isotope, k_L, divided by the rate constant of the heavy isotope, k_H (Eq. (11)).

$$KIE = \frac{1}{\alpha_{p/s}} \tag{10}$$

$$KIE = \frac{k_L}{k_H} \tag{11}$$

Formally, $\alpha_{p/s}$ is defined as the isotopic ratio of instantaneously produced product (R_{pi}) divided by the isotopic ratio of residual substrate at the same instant (R_s) (Eq. (12)).

$$\alpha_{p/s} = \frac{\frac{^{15}N^{pi}}{^{14}N^{pi}}}{\frac{^{15}N^{s}}{^{14}N^{s}}} = \frac{R_{pi}}{R_s} \tag{12}$$

As noted above, the fractionation factor can also be expressed in per mil (‰) terms by using Eq. (1) to convert α to the per mil enrichment factor, ε.

2.3 Assumptions

We used the Rayleigh equation (Eq. (2)) to determine $\alpha_{N\text{-bulk}}$, the fractionation factor for N^{bulk}. The Rayleigh model depends on five key assumptions:

2.3.1 Assumption 1

The reaction is irreversible and occurs in a closed system in the absence of side-reactions (Mariotti et al., 1981).

This means that the final $\delta^{15}N^{bulk}$ value is equal to the initial $\delta^{15}N^s$ value ($\delta^{15}N^{s0}$).

$$\delta^{15}N^{bulk,final} = \delta^{15}N^{s0} \tag{13}$$

2.3.2 Assumption 2

The bulk fractionation factor ($\alpha_{p/s}$ or $\alpha_{N\text{-bulk}}$) is constant.

This means that the isotopic ratio of bulk N produced in an infinitely short time period ($R_{bulk,i}$) divided by the isotopic ratio of the remaining substrate (R_s) is constant (Eq. (14)) (Mariotti et al., 1981).

$$\alpha_{N-bulk} = \frac{R_{bulk,i}}{R_s} \tag{14}$$

150   This assumption should be valid as long as the rate-limiting step of the chemical transformation in question remains the same.

2.3.3 Assumption 3

The light isotope (^{14}N) is much more abundant than the heavy isotope (^{15}N), which is true for all experiments performed with ^{15}N at or near natural abundance.

    This assumption was employed by Mariotti and colleagues to approximate total N abundance ($^{14}N + {}^{15}N$) as ^{14}N in

155   their definition of f (Mariotti et al., 1981). For N_2O isotopocules, the assumption that $^{14}N >> {}^{15}N$ also means that variations in apportionment of ^{15}N between the α and β positions will not significantly affect the abundance of ^{14}N at the α or β position. Thus, at or near natural abundance of ^{15}N, both $^{14}N^{\alpha}$ and $^{14}N^{\beta}$ may be approximated as $0.5*{}^{14}N^{bulk}$. This approximation underlies the assumption that $\delta^{15}N^{bulk}$ is approximately equal to the average of $\delta^{15}N^{\alpha}$ and $\delta^{15}N^{\beta}$ (Eq. (15)).

$$\delta^{15}N^{bulk} = \frac{1}{2} * (\delta^{15}N^{\alpha} + \delta^{15}N^{\beta}) \tag{15}$$

160   Equation 15 is routinely used in isotopic studies of N_2O to calculate $\delta^{15}N^{\beta}$ values using experimentally determined $\delta^{15}N^{bulk}$ and $\delta^{15}N^{\alpha}$ values (Toyoda and Yoshida, 1999).

2.3.4 Assumption 4

The values of δ_{s0} and δ_s are relatively close to 0‰.

    Mariotti's approximation of the Rayleigh equation uses a simplification that is only valid if $\delta_s/1000$ and $\delta_{s0}/1000$ are

165   small relative to 1 (Mariotti et al., 1981). In practice, for an N_2O synthesis reaction where ε_{N-bulk} is -20‰, a $\delta^{15}N^{s0}$ value of ± 100‰ will introduce an error of ~2‰ when ε_{N-bulk} is determined using this approximation (Table S1).

2.3.5 Assumption 5

The absolute value of ε (*e.g.*, ε_{N-bulk}) is relatively small.

    The magnitude of $\delta^{15}N^s$ values depend on both $\delta^{15}N^{s0}$ and ε_{N-bulk}. Thus, similar to the previous assumption, this

170   assumption was introduced to facilitate the approximation that $\delta^{15}N^s/1000$ is small relative to 1 (Mariotti et al., 1981). As with assumption 4, the error introduced by this approximation increases as the absolute value of ε increases. For a reaction where $\delta^{15}N^{s0}$ is equal to 0‰ and ε_{N-bulk} is equal to ±50‰, this approximation introduces an error of ~1‰ to ε values (ε_{N-bulk}, $\varepsilon_{N-\alpha}$, and $\varepsilon_{N-\beta}$) while a reaction where ε_{N-bulk} is equal to ±100‰ introduces an error of 5-6‰ (Table S2).

2.3.6 Assumption 6

175 For the purposes of modeling N_2O synthesis, we will use all of the well-established assumptions listed above. Additionally, to account for fractionation at N^α and N^β individually, we introduce one more assumption:

The individual fractionation factors for the α and β nitrogen atoms in N_2O ($\alpha_{N-\alpha}$ and $\alpha_{N-\beta}$) are essentially constant.

We define $\alpha_{N-\alpha}$ and $\alpha_{N-\beta}$ in a manner analogous to that of α_{N-bulk} (Eq. (14)). Thus, $\alpha_{N-\alpha}$ is defined as the isotopic ratio of N^α from instantaneously produced N_2O ($R_{\alpha,i}$) divided by R_s (Eq. (16)).

$$\alpha_{N-\alpha} = \frac{\frac{15_N\alpha,i}{14_N\alpha,i}}{\frac{15_Ns}{14_Ns}} = \frac{R_{\alpha,i}}{R_s} \tag{16}$$

Similarly, $\alpha_{N-\beta}$ is defined as the instantaneous isotopic ratio of N^β ($R_{\beta,i}$) divided by R_s (Eq. (17)).

$$\alpha_{N-\beta} = \frac{\frac{15_N\beta,i}{14_N\beta,i}}{\frac{15_Ns}{14_Ns}} = \frac{R_{\beta,i}}{R_s} \tag{17}$$

Put another way, we assume *a priori* that the processes that govern preferential incorporation of one isotope over another remain unchanged at both the α and β positions of N_2O during the course of the reaction. We expect this assumption to be

185 valid throughout the reaction, as long as the rate-limiting steps of N_2O biosynthesis are unchanged.

2.4 The standard Rayleigh model and simulation of error-free $\delta^{15}N^{bulk}$ and $\delta^{15}N^s$ values

To compare the standard Rayleigh approach and our nonlinear expansion of the Rayleigh model, we simulated isotopic data for a number of different combinations of kinetic isotope effects for N^α and N^β (see Table 1 and Fig. 1). Each idealized, error-free dataset had three groups of equally spaced values of f (0.7-0.2), similar to a typical experiment with three replicates

190 (Tables S4-S8). For each dataset, $\delta^{15}N^{s0}$ was set at 0‰, and ε_{N-bulk} was set at either -20‰ (normal KIE) or +20‰ (inverse KIE). Equation 2, Mariotti's approximation of the Rayleigh model for accumulated product (Mariotti et al., 1981) was used to calculate $\delta^{15}N^{bulk}$ values of N_2O for each value of f ($\delta^{15}N^{bulk} = \delta^{15}N^p$). Similarly, δ values for remaining substrate ($\delta^{15}N^s$) were calculated using Eq. (18), Mariotti's approximation of the Rayleigh model written in terms of substrate (Mariotti et al., 1981).

195 $$\delta^{15}N^s = \delta^{15}N^{s0} + \varepsilon_{N-bulk} * \ln(f) \tag{18}$$

The $\delta^{15}N^{bulk}$ and $\delta^{15}N^s$ values simulated using the standard Rayleigh equation are shown in Fig. 1 in gray and orange, respectively.

Modeling was performed with R statistical software (R Core Team, 2022), and figures were produced with ggplot2 (Wickham, 2016).

2.5 Nonlinear expansion of the Rayleigh model

Simulated $\delta^{15}N^\alpha$ and $\delta^{15}N^\beta$ values were calculated based on the assumption that, like the fractionation factor for bulk N, the fractionation factors for the individual N^α and N^β atoms are constant (see Assumption 6 above). To relate $\alpha_{N-\alpha}$ and $\alpha_{N-\beta}$ to α_{N-bulk}, we define the fraction of instantaneously converted $^{15}N^{bulk}$ ($^{15}N^{bulk,i}$) that is incorporated into the α position as ρ (Eq. (19)).

$$\rho = \frac{^{15}N^{\alpha,i}}{^{15}N^{bulk,i}} \tag{19}$$

Similarly, we define the fraction of instantaneously converted ^{14}N ($^{14}N^{bulk,i}$) that goes to the α position as τ (Eq. (20)).

$$\tau = \frac{^{14}N^{\alpha,i}}{^{14}N^{bulk,i}} \tag{20}$$

In keeping with the premise that $\alpha_{N-\alpha}$ and $\alpha_{N-\beta}$ are constant, we assume *a priori* that ρ and τ are constant. Thus, the equation for $\alpha_{N-\alpha}$ may be written in terms of ρ, τ, and α_{N-bulk}:

$$\alpha_{N-\alpha} = \frac{\frac{\rho * {}^{15}N^{bulk,i}}{\tau * {}^{14}N^{bulk,i}}}{\frac{^{15}N^S}{^{14}N^S}} = \frac{\rho}{\tau} * \alpha_{N-bulk} \tag{21}$$

In the absence of side-reactions, $^{15}N^{bulk,i}$ must be equal to the sum of $^{15}N^{\alpha,i}$ and $^{15}N^{\beta,i}$. Similarly, $^{14}N^{bulk,i}$ must be equal to the sum of $^{14}N^{\alpha,i}$ and $^{14}N^{\beta,i}$. Thus, the equation for $\alpha_{N-\beta}$ may also be written in terms of ρ, τ, and α_{N-bulk}:

$$\alpha_{N-\beta} = \frac{\frac{(1-\rho) * {}^{15}N^{bulk,i}}{(1-\tau) * {}^{14}N^{bulk,i}}}{\frac{^{15}N_S}{^{14}N_S}} = \frac{1-\rho}{1-\tau} * \alpha_{N-bulk} \tag{22}$$

Equations 21 and 22 form the basis for the Expanded Rayleigh model.

To simulate $\delta^{15}N^\alpha$ and $\delta^{15}N^\beta$ values and determine the corresponding fractionation factors, ρ and τ must be related to accumulated isotope ratios, R_α and R_β. Although ρ is formally defined in Eq. (19) as the fraction of instantaneously converted ^{15}N apportioned to the α position, ρ can also be written in terms of *accumulated* ^{15}N values as long as ρ is constant:

$$\rho = \frac{^{15}N^\alpha}{^{15}N^{bulk}} \tag{23}$$

Similarly, as long as τ is constant, τ may be written in terms of accumulated ^{14}N values:

$$\tau = \frac{^{14}N^\alpha}{^{14}N^{bulk}} \tag{24}$$

Using the definition of ρ from Eq. (23), R_α can be written in terms of ρ by substituting $^{15}N^\alpha$ with $\rho * {}^{15}N^{bulk}$ and replacing $^{14}N^\alpha$ with $0.5*(N^{bulk}) - {}^{15}N^\alpha$ (Eq. (25)).

$$R_\alpha = \frac{^{15}N^\alpha}{^{14}N^\alpha} = \frac{\rho * {}^{15}N^{bulk}}{0.5 * N^{bulk} - \rho * {}^{15}N^{bulk}} \tag{25}$$

The same approach can be used to define R_β in terms of ρ (Eq. (26)).

$$R_\beta = \frac{^{15}N^\beta}{^{14}N^\beta} = \frac{(1-\rho)*^{15}N^{bulk}}{0.5*N^{bulk}-(1-\rho)*^{15}N^{bulk}} \tag{26}$$

225   The term $0.5*N^{bulk}$ is equal to moles of N$_2$O (Eq. (7)), and $^{15}N^{bulk}$ can be calculated for any value of f using N^{bulk} and $\delta^{15}N^{bulk}$ (see SI). Equations 25 and 26 can be converted to δ notation as follows (see Eq. (6)):

$$\delta^{15}N^\alpha = \left(\frac{\rho*^{15}N^{bulk}}{(0.5*N^{bulk}-\rho*^{15}N^{bulk})*R_{standard}} - 1\right) * 1000 \tag{27}$$

$$\delta^{15}N^\beta = \left(\frac{(1-\rho)*^{15}N^{bulk}}{(0.5*N^{bulk}-(1-\rho)*^{15}N^{bulk})*R_{standard}} - 1\right) * 1000] \tag{28}$$

Equations 27 and 28 can be used to determine $\delta^{15}N^\alpha$ and $\delta^{15}N^\beta$ based on $\delta^{15}N^{bulk}$ as long as ρ is constant and $\delta^{15}N^{bulk}$ can be

230   approximated as the average of $\delta^{15}N^\alpha$ and $\delta^{15}N^\beta$ (see Eq. (15) and Table S3).

2.6 Simulation of error-free $\delta^{15}N^\alpha$ and $\delta^{15}N^\beta$ values

Idealized, error-free $\delta^{15}N^\alpha$ and $\delta^{15}N^\beta$ values were simulated for the values of ρ listed in Table 1 by calculating $\delta^{15}N^\alpha$ and $\delta^{15}N^\beta$ using Eq. (27) and Eq. (28) (Tables S4-S8). As outlined in Table 1, five different scenarios with different combinations of isotope effects (none, normal, or inverse) for the α and β nitrogen atoms of N$_2$O were simulated. For Datasets 1 and 5, either

235   $\varepsilon^{15}N^\alpha$ or $\varepsilon^{15}N^\beta$ was set to 0‰ (no isotope effect, KIE = 1), and the corresponding values of ρ and τ were back-calculated (see SI for details). The remaining values of ρ were chosen to produce datasets with the different combinations of normal and/or inverse isotope effects (Datasets 2-4). The ρ values tested (0.4898-0.5200) are all close enough to 0.5 such that the average of $\delta^{15}N^\alpha$ and $\delta^{15}N^\beta$ is approximately equal to $\delta^{15}N^{bulk}$ (Table S3). In all cases, discrepancies between $\delta^{15}N^{bulk}$ values calculated using Eq. (2) and $\delta^{15}N^{bulk}$ values calculated by averaging $\delta^{15}N^\alpha$ and $\delta^{15}N^\beta$ (Eq. (15)) are well below the typical analytical error

240   of 0.5-0.7‰ (Yang et al., 2014).

Modeling was performed with R statistical software (R Core Team, 2022), and figures were produced with ggplot2 (Wickham, 2016).

Table 1. Parameters for idealized, error-free datasets describing N₂O synthesis for five simulated scenarios (Datasets 1-5) with varying combinations of $\varepsilon_{\text{N-bulk}}$ and ρ.

Simulated dataset	Subset	$\varepsilon_{\text{N-bulk}}$ (‰)	δ_{s0} (‰)	ρ [a]	τ [b]
1	$0.3 \leq f \leq 0.7$	-20	0	0.5102	0.49996
2	$0.3 \leq f \leq 0.7$	-20	0	0.5050	0.49998
3	$0.3 \leq f \leq 0.7$	-20	0	0.5200	0.49993
4	$0.3 \leq f \leq 0.7$	20	0	0.5050	0.49998
5	$0.3 \leq f \leq 0.7$	-20	0	0.4898	0.50004

245

[a] Parameter introduced in the Expanded Rayleigh model (Eq. (23)): $\rho = {}^{15}N^{\alpha}/{}^{15}N^{\text{bulk}}$.

[b] Parameter introduced in the Expanded Rayleigh model (Eq. (24)): $\tau = {}^{14}N^{\alpha}/{}^{14}N^{\text{bulk}}$. τ was calculated for each value of f; the average value of τ is listed.
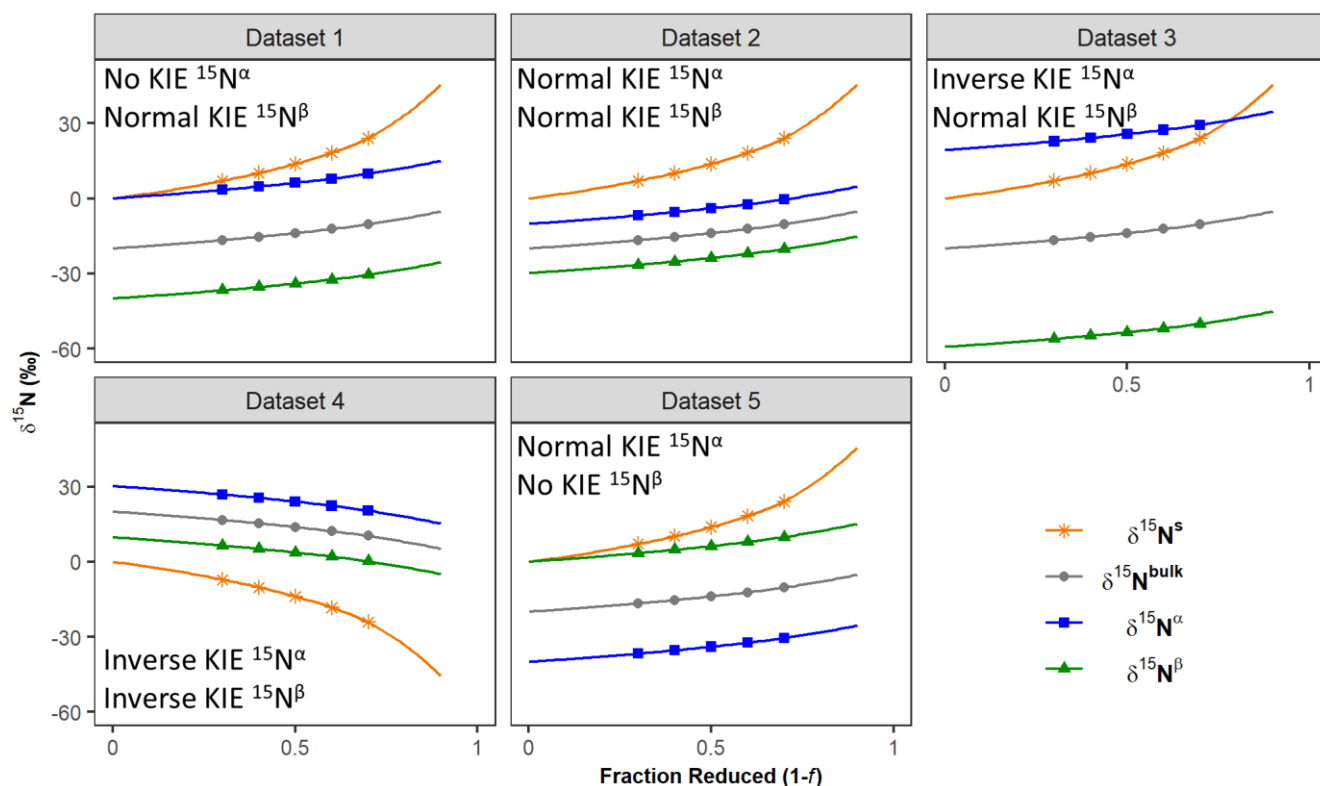
Figure 1. Simulated $\delta^{15}N$ values for N$_2$O synthesis in a closed system with different combinations of KIE $^{15}N^{\alpha}$ and KIE $^{15}N^{\beta}$.

$\delta^{15}N$ values of remaining substrate ($\delta^{15}N^s$) and accumulated product (N$_2$O) ($\delta^{15}N^{bulk}$, $\delta^{15}N^{\alpha}$, and $\delta^{15}N^{\beta}$) are plotted as a function of the fraction of substrate reduced (1-f) with reactions progressing from left to right. Values of $\delta^{15}N^{bulk}$ and $\delta^{15}N^s$ were calculated using Eq (2) or Eq (18) (Mariotti's approximation of the Rayleigh equation (Mariotti et al., 1981)), where $\varepsilon^{15}N^{bulk}$ is set to -20‰ (Datasets 1-3, 5) or +20‰ (Dataset 4) and the initial $\delta^{15}N^s$ value ($\delta^{15}N^{s0}$) is set to 0‰. Values of $\delta^{15}N^{\alpha}$ and $\delta^{15}N^{\beta}$ were calculated using Eq. (27) and Eq. (28). For Datasets 1 and 5, either $\varepsilon^{15}N^{\alpha}$ or $\varepsilon^{15}N^{\beta}$ was set to 0‰ (no isotope effect, KIE = 1), and the corresponding value of ρ was back-calculated (see SI for details). For Datasets 2-4, values of $\delta^{15}N^{\alpha}$ and $\delta^{15}N^{\beta}$ were calculated using pre-determined values of ρ that were less than (Datasets 2 and 4) or greater than (Dataset 3) the value of ρ from Dataset 1. See Table 3 for the KIE values for each simulation.

2.7 Determination of ρ and τ for the Expanded Rayleigh model

To determine $\alpha_{N-\alpha}$ and $\alpha_{N-\beta}$ using Eq. (21) and Eq. (22), ρ and τ must be calculated using values that can be measured experimentally. Because the abundance of ^{14}N is so much greater than that of ^{15}N, variations in ^{15}N apportionment between N^{α} and N^{β} are negligible when determining the fraction of $^{14}N^{bulk}$ at the α position (*i.e.*, τ). For enzyme-catalyzed N$_2$O synthesis with substrate at or near natural abundance of ^{15}N, we have found that τ is always 0.5000 (see analysis of data from Sutka et al., 2006 (below) (Sutka et al., 2006) and Yang et al., (Yang et al., 2014)). For the purposes of testing our new Expanded

Rayleigh model, we calculated more precise values of τ. To do this, τ was calculated for each value of f using Eq. (24), and the average τ value for each Dataset was used to calculate fractionation factors.

To determine ρ using values that can be measured experimentally, Eq. (15) is rewritten so that ρ is the only unknown parameter. This can be accomplished by replacing $\delta^{15}N^{\alpha}$ with the equivalent term from Eq. (27), producing Eq. (29), a nonlinear equation

270   we have named nonlinear model 1.

$$\delta^{15}N^{bulk} = \frac{1}{2} * \left[\left(\frac{\rho * {}^{15}N^{bulk}}{(0.5*N^{bulk} - \rho*{}^{15}N^{bulk})*R_{standard}} - 1 \right) * 1000 + \delta^{15}N^{\beta} \right] \tag{29}$$

Alternatively, $\delta^{15}N^{\beta}$ could be replaced with a term that includes ρ (Eq. (28)), producing Eq. (30) (nonlinear model 2):

$$\delta^{15}N^{bulk} = \frac{1}{2} * \left[\delta^{15}N^{\alpha} + \left(\frac{(1-\rho)*{}^{15}N^{bulk}}{(0.5*N^{bulk} - (1-\rho)*{}^{15}N^{bulk})*R_{standard}} - 1 \right) * 1000 \right] \tag{30}$$

Both nonlinear models were used to find the optimal value of ρ via nonlinear least squares regression for each of our simulated

275   datasets. Nonlinear least squares regression was performed as previously described (Baty et al., 2015) using a starting ρ value of 0.5.
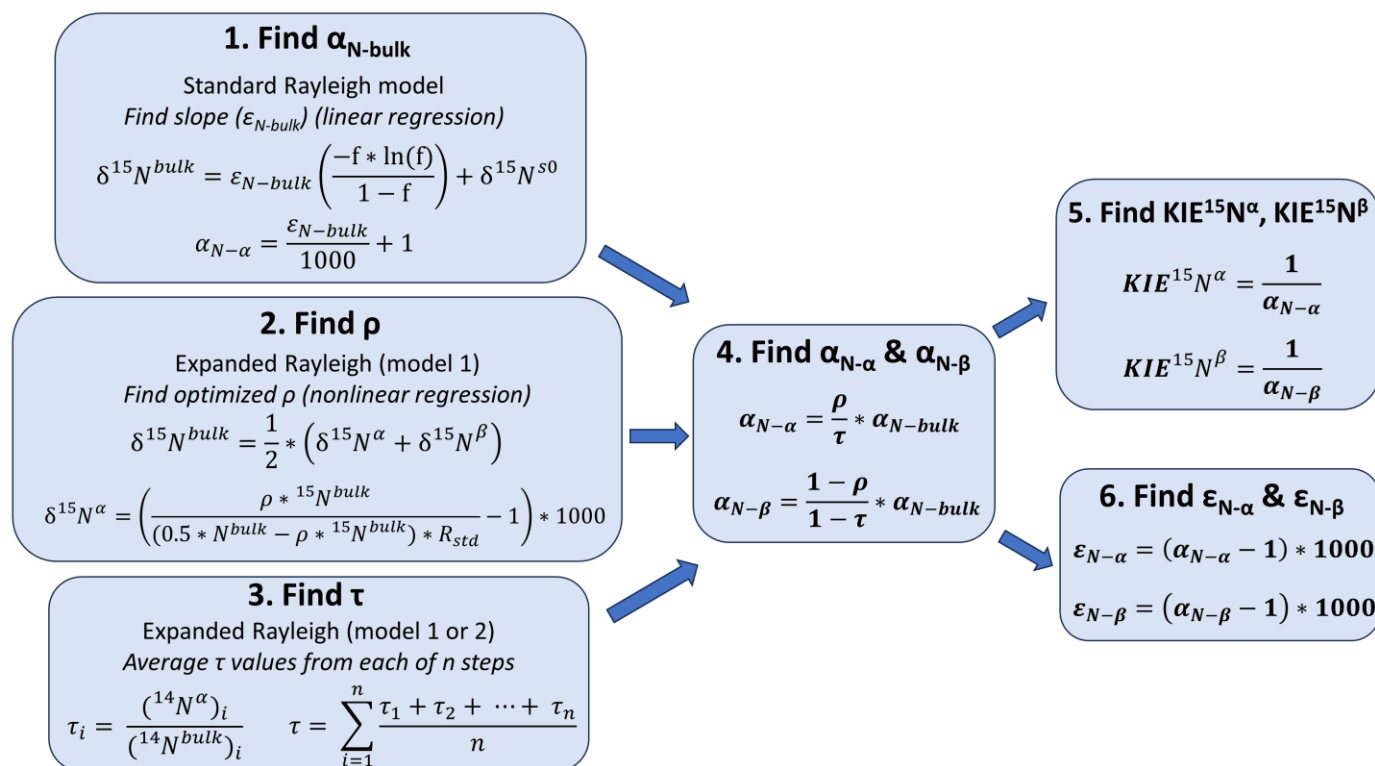
Figure 2. General workflow for using the Expanded Rayleigh model to determine fractionation factors (α) and kinetic isotope effects (KIEs) for the individual N atoms (N$^\alpha$ and N$^\beta$) in N$_2$O.

To determine the fractionation factors for the α and β atoms in N$_2$O ($\alpha_{N-\alpha}$ and $\alpha_{N-\beta}$), three separate values must be calculated. 1. The fractionation factor for bulk N (α_{N-bulk}) is determined by finding the slope (ε_{N-bulk}) of a standard Rayleigh plot where y = [-flnf/(1-f)] and x = $\delta^{15}N^{bulk}$ and converting ε_{N-bulk} to α_{N-bulk} as has been previously described (Mariotti et al., 1981). 2. Nonlinear modeling is used to determine the optimal value of ρ (the fraction of $^{15}N^{bulk}$ at the α position). For Expanded Rayleigh model 1 (shown here), $\delta^{15}N^\alpha$ is replaced in the top equation with an equivalent expression that includes ρ (bottom equation) to generate the model used for nonlinear least squares regression (Eq. (29)). For Expanded Rayleigh model 2, $\delta^{15}N^\beta$ is substituted, producing Eq. (30) (not shown). 3. The value of τ (the fraction of $^{14}N^{bulk}$ at the α position) is determined by dividing $^{14}N^\alpha$ by $^{14}N^{bulk}$ for each step of the reaction and averaging the results. 4. Finally, α_{N-bulk}, ρ, and τ are used to calculate $\alpha_{N-\alpha}$ and $\alpha_{N-\beta}$. 5-6. These individual fractionation factors can be converted to the corresponding KIE values (Eq. (10)) or ε values (Eq (1)).

2.8 Generation of datasets with simulated error

To mimic experimental error, 1000 simulated datasets were generated from each error-free dataset by adding random error to N^s, $\delta^{15}N^{bulk}$, and $\delta^{15}N^\alpha$ using a modified version of the procedure outlined by Scott and colleagues (Scott et al., 2004). Error was propagated to f by recalculating f using the N^s values with error added (f = N^s / N^{s0}). Similarly, error was propagated to $\delta^{15}N^\beta$ by recalculating $\delta^{15}N^\beta$ using $\delta^{15}N^{bulk}$ and $\delta^{15}N^\alpha$ values with error added (Eq. (15)). For each simulation, fractionation factors and KIE values were calculated using the standard Rayleigh model and the Expanded Rayleigh model (versions 1 and

2), and the KIE values from each set of 1000 simulations were averaged. Three "levels" of error (low, medium, and high) and three types of skewness (none, left-skewed, and right-skewed, see below) were used for a total of nine conditions (Table 2, Fig. 3, and Figs. S1-S4). For simulations with low error, the standard deviation of each randomly generated error term was set

300   to the level of error expected in a typical experiment (Table 2). The standard deviation of N^s values was set to 1.5% of N^{s0} (the maximum value of N^s), which corresponds to the estimated level of error in gas volume measurements (see SI). The standard deviations of $\delta^{15}N^{bulk}$ and $\delta^{15}N^{\alpha}$ were set to 0.5‰ and 0.7‰, respectively, which correspond to standard deviations typical for isotopic analysis of N_2O via IRMS (Yang et al., 2014). To further test the robustness of the linear and nonlinear models, medium- and high-level error terms were generated by multiplying the low-level error terms for N^s, $\delta^{15}N^{bulk}$, and $\delta^{15}N^{\alpha}$ by the

305   appropriate factor (Table 2). The multiplication factors for medium- and high-level error were chosen so that the average R^2 values produced by linear regression of $\delta^{15}N^{bulk}$ against [-flnf/(1-f)]) were approximately 0.7 and 0.4, respectively. Similar R^2 values have been observed for standard Rayleigh linear regression plots for N_2O biosynthesis (*e.g.*, (Yang et al., 2014), Figs. S2-S4).

310   **Table 2. Standard deviation and skewness of random error added to simulated N^s, $\delta^{15}N^{bulk}$, and $\delta^{15}N^{\alpha}$ values.**

Level of error[a]	N^s (nmol)	$\delta^{15}N^{bulk}$ (‰)	$\delta^{15}N^{\alpha}$ (‰)	Skewness[b]	
Low	0.015*N^{s0} [c]	0.5	0.7	None	|Skewness| ≤ 0.5
				Left	Skewness < -0.5
				Right	Skewness > 0.5
Medium	2*(0.015*N^{s0}) [c]	2.5*(0.5)	2.5*(0.7)	None	|Skewness| ≤ 0.5
				Left	Skewness < -0.5
				Right	Skewness > 0.5
High	3*(0.015*N^{s0}) [c]	5*(0.5)	5*(0.7)	None	|Skewness| ≤ 0.5
				Left	Skewness < -0.5
				Right	Skewness > 0.5

[a] "Level of error" refers to the standard deviations of N^s (nmol of remaining substrate), $\delta^{15}N^{bulk}$, and $\delta^{15}N^{\alpha}$.

[b] Skewness of the residuals for the standard Rayleigh model (linear regression of $\delta^{15}N^{bulk}$ against [-flnf/(1-f)]).

[c] N^{s0} refers to nmol of substrate at time = 0 (*i.e.*, the maximum amount of substrate). N^{s0} was set to 10,000 nmol in all

315   simulations.

For each level of error, three sets of 1000 simulations with different types of skewness (no skew, left-skewed, or right-skewed) were performed to mimic types of skewness that might be observed in experimental data. For example, if N_2O leaks from a sample bottle prior to analysis, the quantity of N_2O produced will be underestimated, and the corresponding

320 values of N^s and f will be overestimated. Additionally, since light isotopes have a higher rate of both diffusion and effusion, values of $\delta^{15}N^{bulk}$, $\delta^{15}N^{\alpha}$, and $\delta^{15}N^{\beta}$ will be overestimated. This scenario is represented by simulations where the random error values added to N^s, $\delta^{15}N^{bulk}$, and $\delta^{15}N^{\alpha}$ were derived from left-skewed distributions. Skewness classifications were then assigned based on the skewness of the residuals for the standard Rayleigh model where the dependent variable (y) is $\delta^{15}N^{bulk}$ (Table 2). Simulations with residuals between -0.5 and 0.5 (inclusive) were designated "no skew," meaning the distribution

325 of these residuals did not differ significantly from the normal distribution. Simulations where standard Rayleigh residuals had a skewness value less than -0.5 were designated "left-skewed" (*i.e.*, left-tailed distribution), and simulations where skewness was greater than 0.5 were designated "right-skewed" (*i.e.*, right-tailed distribution). The skewness function from the moments package in R was used to calculate skewness values (Komsta and Novomestky, 2022). In this package, skewness is defined as $(1/n)*\Sigma((x - \overline{x})/s)^3$, where n is the sample size, $\overline{x}$ is the sample mean, and s is the sample standard deviation (Hippel, 2011),

330 To assess the accuracy of each model under different circumstances, average KIE values and standard deviations were calculated for each set of 1000 simulations with error. The absolute relative difference of each average KIE was calculated by finding the absolute value of the difference of the estimate (average KIE) and the actual value divided by the actual value (Eq. (31)).

$$absolute\ relative\ difference = |\frac{estimate-actual}{actual}| \tag{31}$$

335 Actual values were calculated directly from the input values for simulations without error (see Table 3). Lower absolute relative difference values indicate higher accuracy. Goodness of fit was assessed for the (linear) standard Rayleigh model and nonlinear models 1 and 2 by calculating the average root mean square error (RMSE) for each set of 1000 simulations. For each simulation, p-values for $\varepsilon_{N\text{-}bulk}$ and ρ (coefficients extracted from the (linear) standard Rayleigh model and nonlinear models 1 or 2, respectively) were determined using the one-sample *t*-test (two-sided) (Baty et al., 2015; Ritz and Streibig,

340 2008; Kalpić et al., 2011). The null hypothesis used to calculate these p-values is that there is no kinetic isotope effect. For the linear model, this means that the null hypothesis is $\varepsilon_{N\text{-}bulk} = 0$ (KIE $^{15}N^{bulk} = 1$). For the nonlinear models, the null hypothesis is that $\rho = 0.5$ (KIE $^{15}N^{\alpha} = 1$ and KIE $^{15}N^{\beta} = 1$).

Modeling and statistical analyses were performed with R statistical software (R Core Team, 2022), random numbers representing simulated error were generated using the rsn function from the skew-normal distribution package (Azzalini,

345 2023), skewness was calculated with the moments package (Komsta and Novomestky, 2022), and figures were produced with ggplot2 (Wickham, 2016).
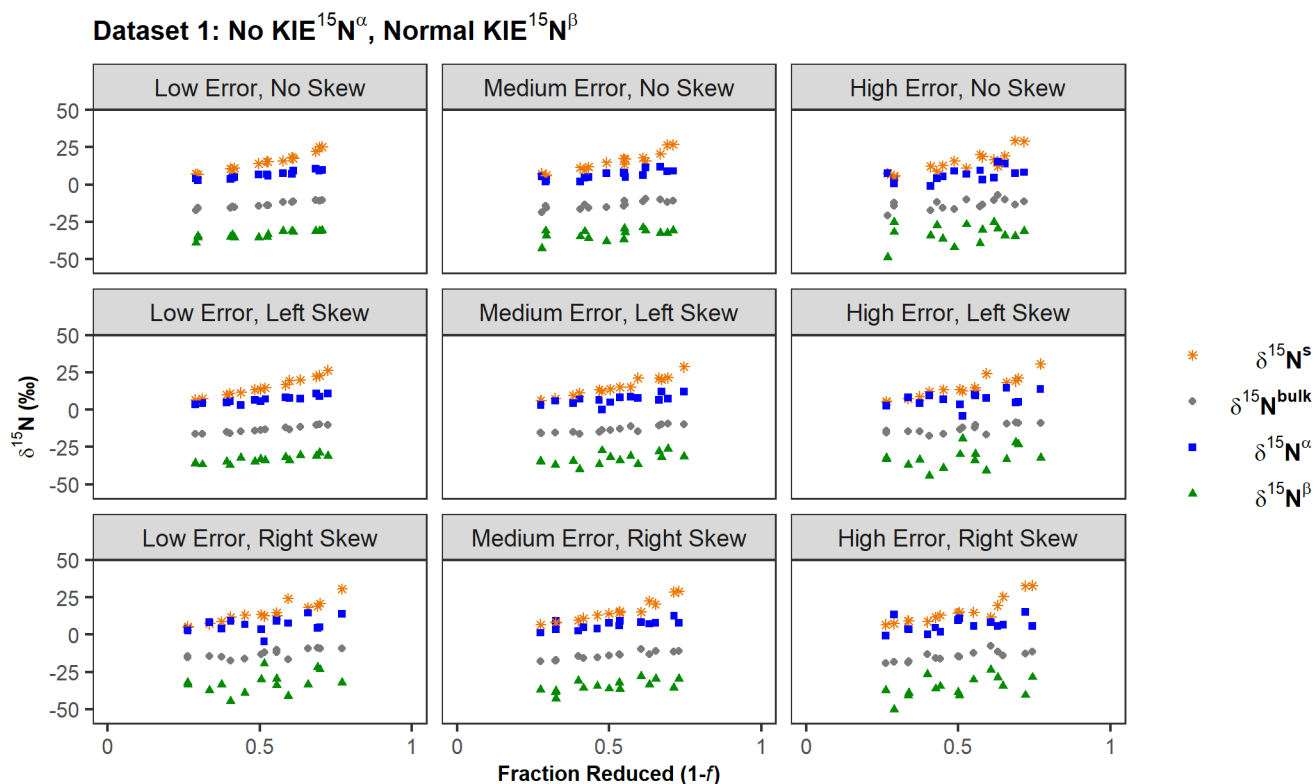
Figure 3. Example simulations derived from Dataset 1 with varying levels of error and types of skewness.

Each panel shows a single dataset (representative of 1000 simulated datasets) consisting of three replicates with five timepoints each.
All simulations were derived from Dataset 1 ($\delta^{15}N^{s0} = 0‰$, $\varepsilon_{\text{N-bulk}} = -20‰$, KIE $^{15}N^{\alpha} = 1.0000$, and KIE $^{15}N^{\beta} = 1.0417$). Each level of
error and type of skewness is described in Table 2. Example graphs derived from Datasets 2-4 are shown in Figs. S1-S4.

2.9 Analysis of previously published experimental data

The standard and Expanded Rayleigh models were applied to published data on N$_2$O produced from NH$_2$OH by *Methylosinus*
trichosporium (ATCC 49243) (Sutka et al., 2006). We calculated values of f, $\delta^{15}N^{\alpha}$, and $\delta^{15}N^{\beta}$ using the N$_2$O concentrations,
$\delta^{15}N^{\text{bulk}}$ values, and site preference (SP) values from replicate B measured by Sutka et al. (see Table S14 for original data and
our calculated values, and Fig. 4 for a graphical representation of these data). SP is defined as the difference between $\delta^{15}N^{\alpha}$
and $\delta^{15}N^{\beta}$:

$$SP = \delta^{15}N^{\alpha} - \delta^{15}N^{\beta} \qquad (32)$$

The data for replicate B was chosen because this data had a range of f values large enough for $\varepsilon_{\text{N-bulk}}$ to be determined via the
standard Rayleigh method (linear regression of $\delta^{15}N^{\text{bulk}}$ against [-flnf/(1-f)]). See SI for details.

We also applied the standard and Expanded Rayleigh models to previously published isotopic data on N$_2$O production
from purified *Histoplasma capsulatum* (fungal) P450 NOR (Fig. 5 and Table S16) (Yang et al., 2014). Because this dataset

covered a wide range of f values (f = 0.42-0.87) and $\delta^{15}N^{bulk}$ varied linearly with [-flnf/(1-f)], we used the standard Rayleigh

model (Eq. (2)) to determine $\varepsilon_{N\text{-}bulk}$ via linear regression of $\delta^{15}N^{bulk}$ against [-flnf/(1-f)]. $\varepsilon_{N\text{-}bulk}$ was determined for each of three

365   independent biological replicates (13 observations/replicate), and the results were averaged. Similarly, to determine standard

Rayleigh values of $\varepsilon_{N\text{-}\alpha}$ and $\varepsilon_{N\text{-}\beta}$, we performed linear regression of $\delta^{15}N^{\alpha}$ or $\delta^{15}N^{\beta}$ against [-flnf/(1-f)] for each independent

replicate and averaged the results.

To apply the Expanded Rayleigh model to the isotopic data on N_2O production by P450 NOR, we used a modified

procedure because, in this case, ρ and τ vary linearly with [-flnf/(1-f)]. Therefore, instead of using nonlinear model 1 (Eq. (29)

370   or model 2 (Eq. (30)) to determine ρ using data from the entire reaction, we calculated ρ for each individual time point (*i.e.*,

each individual value of f) using Eq. (23). Similarly, τ was calculated for each individual observation using Eq. (24). These

individual ρ and τ values were then used to calculate $\alpha_{N\text{-}\alpha}$ (Eq. (21)) and $\alpha_{N\text{-}\beta}$ (Eq. (22)) values for each value of f, which were

then converted to KIE values using Eq. (10). This approach yielded KIE values that increased (KIE $^{15}N^{\alpha}$) or decreased (KIE

$^{15}N^{\beta}$) as the reaction progressed. To estimate the range of position-specific KIEs produced by the Expanded Rayleigh model,

375   individual KIE $^{15}N^{\alpha}$ and KIE $^{15}N^{\beta}$ values representing the early part of the reaction (f = 0.8 ± 0.03) or the latter part of the

reaction (late reaction, f = 0.5 ± 0.03) were averaged (Table 6, Table S17).

Modeling was performed with R statistical software (R Core Team, 2022), and $\delta^{15}N$ values were plotted with ggplot2

(Wickham, 2016). A linear model was used to determine if SP changed as a function of [-flnf/(1-f)].
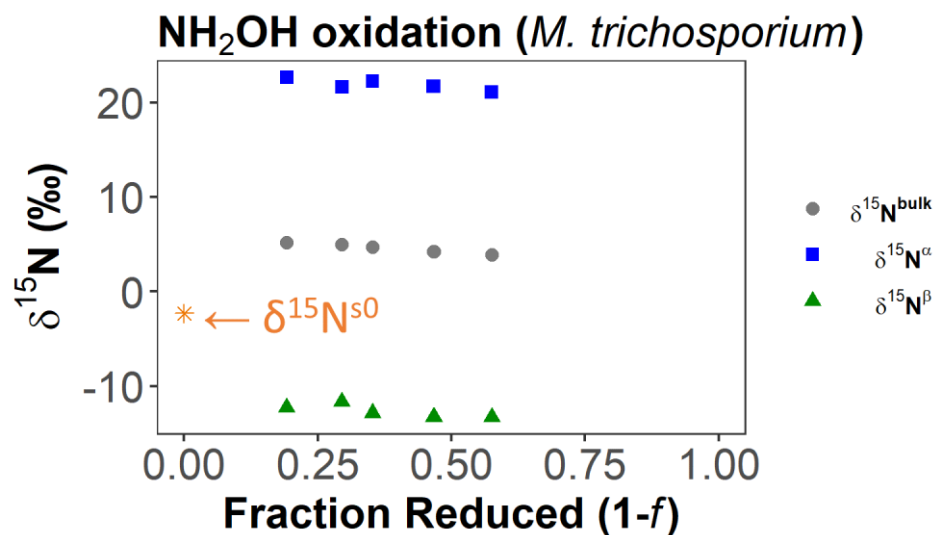
380

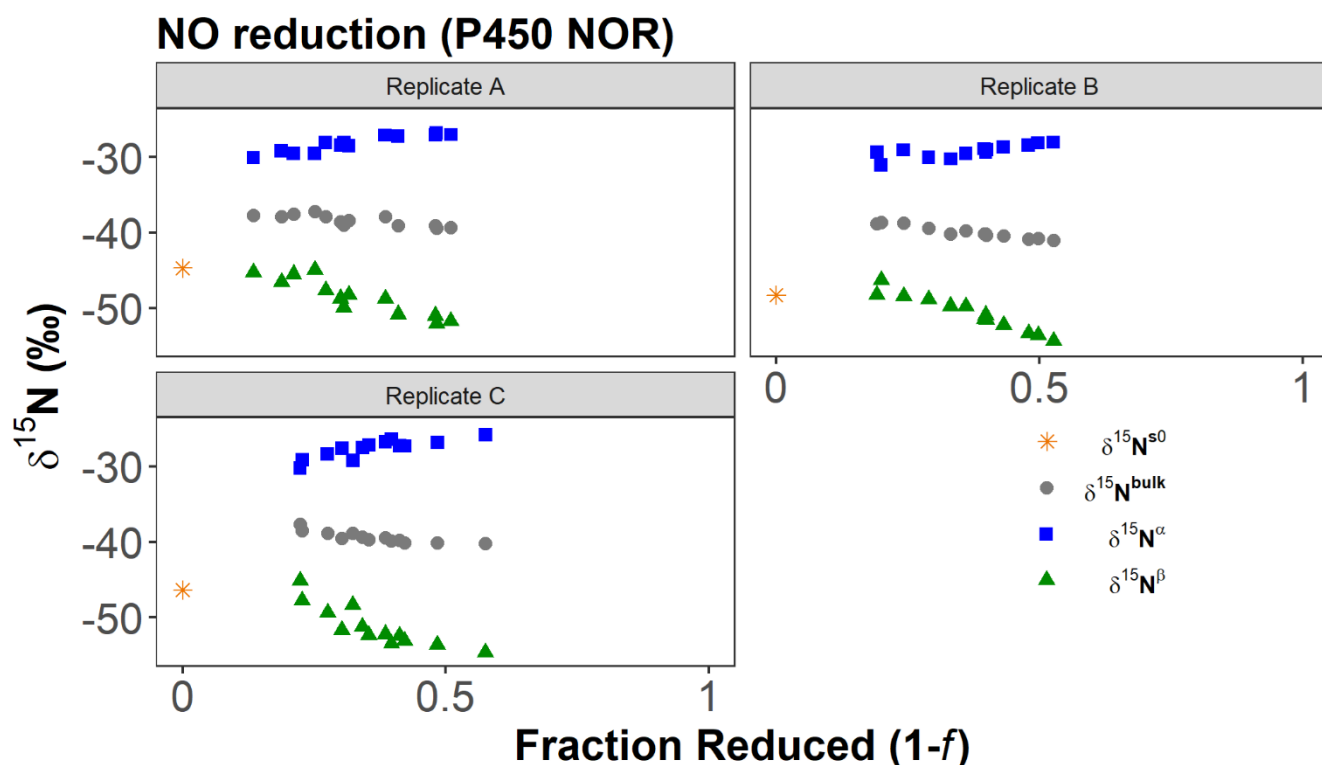**Figure 4. Experimentally measured $\delta^{15}N$ values for N_2O synthesis from NH_2OH in a pure culture of *Methylosinus trichosporium* (data from (Sutka et al., 2006)).**

Data previously reported for *M. trichosporium* (*Methylocystis* sp.) replicate B (Sutka et al., 2006). $\delta^{15}N$ values of accumulated product (N_2O) ($\delta^{15}N^{bulk}$, $\delta^{15}N^{\alpha}$, and $\delta^{15}N^{\beta}$) are plotted as a function of the fraction of substrate reduced (1-f) with the reaction progressing
385 from left to right. We back-calculated values of f, $\delta^{15}N^{\alpha}$, and $\delta^{15}N^{\beta}$ using the reported N_2O concentrations, $\delta^{15}N^{bulk}$ values, and SP values. The initial measured $\delta^{15}N$ value of NH_2OH ($\delta^{15}N^{s0}$), -2.3‰, is shown at f = 1.

Figure 5. Experimentally measured product $\delta^{15}N$ values and calculated $\delta^{15}N^{s0}$ values for N₂O synthesis from NO by purified *H. capsulatum* P450 NOR (data from (Yang et al., 2014)).

Data previously reported for *H. capsulatum* (fungal) P450 NOR replicates A-C (Yang et al., 2014). $\delta^{15}N$ values of accumulated product (N₂O) ($\delta^{15}N^{bulk}$, $\delta^{15}N^{\alpha}$, and $\delta^{15}N^{\beta}$) are plotted as a function of the fraction of substrate reduced (1-f) with the reaction progressing from left to right. We back-calculated $\delta^{15}N^{s0}$ for each replicate by finding the intercept of the corresponding standard Rayleigh plot (Eq. (2)) where x = [-flnf/(1-f)] and y = $\delta^{15}N^{bulk}$.

3 Results

3.1 Error-free simulations

To demonstrate that the standard Rayleigh model produces inaccurate results for the individual nitrogen atoms in N₂O, idealized, error-free datasets were simulated representing different scenarios with varying combinations of KIEs for N$^{\alpha}$ and N$^{\beta}$ (Fig. 1, Table 1). Application of the standard Rayleigh model to each dataset produces KIE $^{15}N^{bulk}$ values that match the actual KIE $^{15}N^{bulk}$ values (calculated by converting the input ε_{N-bulk} value to a KIE value). However, the KIE $^{15}N^{\alpha}$ and KIE $^{15}N^{\beta}$ values determined using the standard Rayleigh approach differ significantly from the actual KIEs calculated from simulation input values (Table 3). In each of the five simulated reactions (Datasets 1-5), the isotopic preference for N$^{\alpha}$ differs from that of N$^{\beta}$, which can be verified visually by noting that the $\delta^{15}N^{\alpha}$ values are significantly different than the $\delta^{15}N^{\beta}$ values throughout each reaction (Fig. 1). However, in all five cases, the standard Rayleigh model produces KIE values for N$^{\alpha}$ and N$^{\beta}$

405 that are approximately equal, highlighting the fact that the standard Rayleigh model inaccurately quantifies KIE $^{15}N^{\alpha}$ and KIE $^{15}N^{\beta}$.

The inadequacies of the standard Rayleigh model are most evident when N^{α} and N^{β} have opposing kinetic isotope effects, *i.e.*, scenarios where there is an inverse isotope effect at one position and a normal isotope effect at the other position (Dataset 3), or when only one position has a non-zero fractionation factor (Datasets 1, 5). In these cases, the standard Rayleigh

410 model fails to predict the correct type of isotope effect for one of the nitrogen atoms. For example, Dataset 1 represents a scenario where there is no isotopic preference at the α position, meaning instantaneous $\delta^{15}N^{\alpha}$ ($\delta^{15}N^{\alpha i}$) is always equal to $\delta^{15}N^s$. Under these circumstances, KIE $^{15}N^{\alpha}$ is equal to 1.0000. However, the standard Rayleigh model predicts a much higher KIE $^{15}N^{\alpha}$ value (1.0208), incorrectly indicating that there is a reasonably strong, *normal* KIE at the α position. The standard Rayleigh KIE $^{15}N^{\beta}$ value calculated for Dataset 1 is also too low (1.0200 instead of 1.0417), underestimating the preference

415 for ^{14}N at the β position. Similarly misleading results are produced for Dataset 5, where there is no isotope effect for N^{β}, but the standard Rayleigh model predicts a normal isotope effect at this position. Along the same lines, the standard Rayleigh KIE values for Dataset 3 incorrectly indicate that both N^{α} and N^{β} have normal isotope effects when, in this case, N^{α} actually has an inverse isotope effect. Thus, even for a simulated dataset with no experimental error, the standard Rayleigh model produces results that are quantitatively—and, sometimes, qualitatively—incorrect.

420

Table 3. KIE values for N^{bulk}, N^{α}, and N^{β} calculated directly from simulation input values (Actual) or from the standard Rayleigh model or Expanded Rayleigh model.

Simulated dataset			Model		
		Actual[a]	Standard Rayleigh[b]	Expanded Rayleigh 1[c]	Expanded Rayleigh 2[c]
1 No KIE $^{15}N^{\alpha}$ Normal KIE $^{15}N^{\beta}$	**KIE $^{15}N^{bulk}$**	1.0204	1.0204	1.0204	1.0204
	KIE $^{15}N^{\alpha}$	1.0000	1.0208	1.0000	1.0000
	KIE $^{15}N^{\beta}$	1.0417	1.0200	1.0417	1.0417
2 Normal KIE $^{15}N^{\alpha}$ Normal KIE $^{15}N^{\beta}$	**KIE $^{15}N^{bulk}$**	1.0204	1.0204	1.0204	1.0204
	KIE $^{15}N^{\alpha}$	1.0103	1.0206	1.0103	1.0103
	KIE $^{15}N^{\beta}$	1.0308	1.0202	1.0308	1.0308
3 Inverse KIE $^{15}N^{\alpha}$ Normal KIE $^{15}N^{\beta}$	**KIE $^{15}N^{bulk}$**	1.0204	1.0204	1.0204	1.0204
	KIE $^{15}N^{\alpha}$	0.9810	1.0212	0.9810	0.9810
	KIE $^{15}N^{\beta}$	1.0631	1.0196	1.0631	1.0631
4 Inverse KIE $^{15}N^{\alpha}$ Inverse KIE $^{15}N^{\beta}$	**KIE $^{15}N^{bulk}$**	0.9804	0.9804	0.9804	0.9804
	KIE $^{15}N^{\alpha}$	0.9706	0.9802	0.9707	0.9706
	KIE $^{15}N^{\beta}$	0.9903	0.9806	0.9903	0.9903
5 Normal KIE $^{15}N^{\alpha}$ No KIE $^{15}N^{\beta}$	**KIE $^{15}N^{bulk}$**	1.0204	1.0204	1.0204	1.0204
	KIE $^{15}N^{\alpha}$	1.0417	1.0200	1.0417	1.0417
	KIE $^{15}N^{\beta}$	1.0000	1.0208	1.0000	1.0000

[a] Actual values were calculated directly from the input values used to generate the dataset.

[b] KIE values were calculated from ε_{N-bulk}, $\varepsilon_{N-\alpha}$, or $\varepsilon_{N-\beta}$ values obtained via linear regression of $\delta^{15}N^{bulk}$, $\delta^{15}N^{\alpha}$, or $\delta^{15}N^{\beta}$ against [-flnf/(1-f)]) (see Eq. (2))

[c] For the Expanded Rayleigh model, α_{N-bulk} was determined with the standard Rayleigh approach, ρ was determined via nonlinear regression (nonlinear model 1 or 2, Eq. (29) or Eq. (30)), and τ was determined by averaging $^{14}N^{\alpha}/^{14}N^{bulk}$ for every step of the reaction.

The standard Rayleigh model produces inaccurate results for the individual N atoms in N_2O because the changes in $\delta^{15}N^{\alpha}$ depend on both KIE $^{15}N^{\alpha}$ and KIE $^{15}N^{\beta}$, as do changes in $\delta^{15}N^{\beta}$. Linear regression of standard Rayleigh plots for $\delta^{15}N^{\alpha}$ or $\delta^{15}N^{\beta}$ fails to capture this nuance. To address this issue, we have developed an expanded version of the Rayleigh model that introduces two new parameters, ρ and τ, to define how $^{15}N^{bulk}$ and $^{14}N^{bulk}$, respectively, are apportioned between N^{α} and N^{β}. Fractionation factors for N^{α} and N^{β} are determined by combining α_{N-bulk}, ρ, and τ (Eq. (21) and Eq. (22)). For experiments conducted at natural abundance of ^{15}N, the value of τ, which is equal to $^{14}N^{\alpha}/^{14}N^{bulk}$, should always be quite close to 0.5, as discussed above. Indeed, each simulated reaction step has a mean value of τ equal to 0.500 for Datasets 1-5 (Tables S9-S13), so the average value of $^{14}N^{\alpha}/^{14}N^{bulk}$ was used to calculate of $\alpha_{N-\alpha}$ and $\alpha_{N-\beta}$. To determine the value of ρ that fits the entire dataset as accurately as possible, we performed nonlinear least squares regression using the formula shown in Eq. (29) (nonlinear

model 1) or Eq. (30) (nonlinear model 2). For error-free Datasets 1-5, nonlinear least-squares regression with either nonlinear

440 model correctly predicted ρ. Combining these ρ and τ values with α_{N-bulk} values derived from the standard Rayleigh equation yields KIE $^{15}N^\alpha$ and KIE $^{15}N^\beta$ values that are identical to the expected values out to three or four decimal places (Table 3). Thus, unlike the standard Rayleigh approach, the Expanded Rayleigh model successfully recapitulates the kinetic isotope effects for N^α and N^β in an error-free dataset.

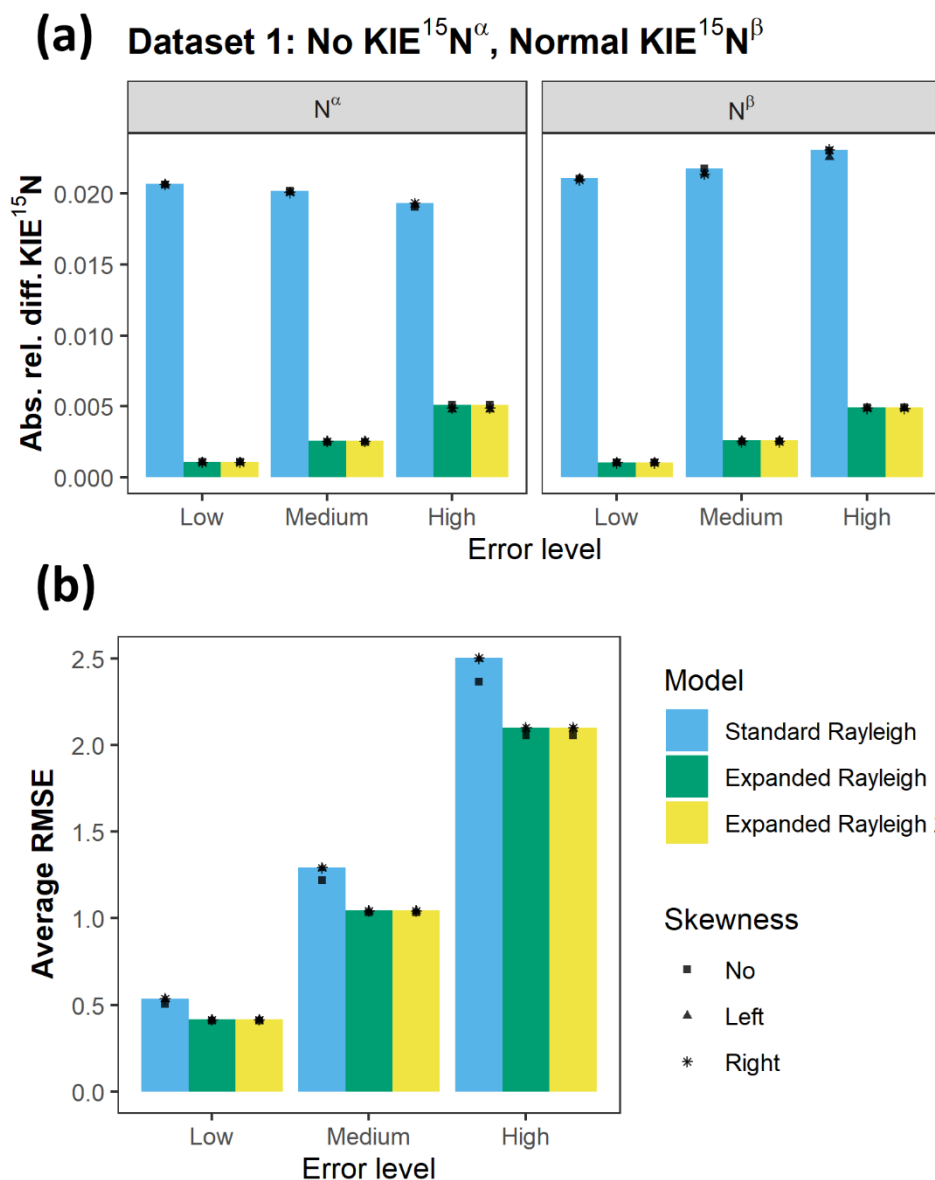**3.2 Application of the Expanded Rayleigh model to simulations with error**

445 To test the robustness of the Expanded Rayleigh model, we applied this model to simulated data with error at varying levels of size and skewness (Table 2) and averaged the results from 1000 simulations for each error category (Table 4, Tables S9-S13). These results indicate that at a low level of error (the level of error expected for a typical experiment), the KIE values produced by the Expanded Rayleigh model are quite accurate (absolute difference relative to true values is 0.001, or 0.1%, see Eq. (31)), regardless of the skewness of the standard Rayleigh model residuals (Fig. 6, Figs. S5-S8). The standard deviations

450 for each average KIE $^{15}N^{bulk}$, KIE $^{15}N^\alpha$, or KIE $^{15}N^\beta$ value (0.0013-0.0014) are also similar to standard error values from typical experiments (~0.0004-0.0021) (Table 5, Table 6) (Sutka et al., 2006; Yang et al., 2014). As the absolute value of the simulated error increases, the average KIE values become less accurate, and the corresponding standard deviations increase. Nonetheless, even at the highest level of error, the maximum absolute relative difference of average KIE values is 0.005 (0.5% difference), and the range of values covered by average KIE ± standard deviation includes the actual KIE value. Thus, the Expanded

455 Rayleigh model provides a robust method for determining KIE values even when the datasets have a high level of error or skewness.

In contrast to the Expanded Rayleigh model, the KIE $^{15}N^\alpha$ and KIE $^{15}N^\beta$ values determined for simulations with error using the standard Rayleigh model alone are much less accurate (Fig. 6, Figs. S5-8). For all simulations derived from Datasets 1-5 at all levels of error and types of skewness, the absolute relative differences of average standard Rayleigh KIE $^{15}N^\alpha$ and

460 KIE $^{15}N^\beta$ values ranged from 0.01-0.04 (1-4% difference). These absolute relative differences are 2-40 times higher than the corresponding differences of Expanded Rayleigh model estimates (Fig. 6, Figs. S5-8). Differences of this magnitude are large enough that the true KIE $^{15}N^\alpha$ and KIE $^{15}N^\beta$ values typically do not fall within the range covered by average KIE ± standard deviation calculated using the standard Rayleigh model (data not shown). Thus, as discussed for the no-error simulations, standard Rayleigh KIE $^{15}N^\alpha$ and KIE $^{15}N^\beta$ values do not accurately quantify isotopic fractionation at the α and β positions of

465 N_2O and can even lead to inaccurate designation of the type of KIE (*i.e.*, no KIE, normal KIE, or inverse KIE) at either N^α or N^β. In short, for all levels of error and types of skewness tested, the standard Rayleigh model is only accurate for bulk N. *To obtain KIE $^{15}N^\alpha$ and KIE $^{15}N^\beta$ values with the same level of accuracy as KIE $^{15}N^{bulk}$, the KIE $^{15}N^{bulk}$ value obtained via the standard Rayleigh model must be combined with ρ and τ, parameters from the Expanded Rayleigh model.*

The error for KIE $^{15}N^\alpha$ and KIE $^{15}N^\beta$ values is derived from three sources: error in α_{N-bulk}, error in ρ, and error in τ. In

470 all of our simulations with added error, the most significant source of error is the error associated with α_{N-bulk}, which is derived

22

from linear regression of $\delta^{15}N^{bulk}$ against [-flnf/(1-f)]. As the level of error increases, the accuracy of ε_{N-bulk} (and thus the accuracy of α_{N-bulk} and KIE $^{15}N^{bulk}$) decreases more significantly than the accuracy of ρ and τ estimates (Tables S9-S13). The same trend is apparent for other assessments of model fit. The RMSE values for the nonlinear regression portion of the Expanded Rayleigh model (1 or 2) are always slightly lower than the RMSE values for the standard Rayleigh linear model

475   (Fig. 6, Figs. S5-S8), indicating that the linear and nonlinear models produce similar "goodness of fit" values. Similarly, the p-values for ε_{N-bulk}, the slope of the linear regression model, are always greater than the p-values for ρ, the coefficient extracted from the nonlinear portion of the Expanded Rayleigh model. (In both cases, the null hypothesis is that KIE = 1; see Methods.) Out of each set of 1000 simulations at high-level error, a small number of simulated datasets (14-19%) produce linear regression plots where confidence in the slope is low (*i.e.*, ε_{N-bulk} p-value > 0.05) (data not shown). In contrast, all of the

480   simulations derived from all five datasets with varying types of KIEs produce ρ values that are likely to be significant (p-value < 0.001). Overall, application of the Expanded Rayleigh model to simulated datasets with varying types of error indicates that this method of determining individual fractionation factors for N^{α} and N^{β} is robust even at high levels of error.

Figure 6. Comparison of the accuracy and goodness of fit of the standard Rayleigh model and Expanded Rayleigh models 1 and 2.

A. Comparison of the accuracy of KIE $^{15}N^\alpha$ and KIE $^{15}N^\beta$ values. For each model, the absolute relative difference for KIE $^{15}N^\alpha$ and KIE $^{15}N^\beta$ values (average for 1000 simulated datasets derived from Dataset 1) are shown. Actual values for Dataset 1: $\delta^{15}N^{s0}$ = 0‰, $\varepsilon_{N\text{-bulk}}$ = -20‰, KIE $^{15}N^\alpha$ = 1.0000, and KIE $^{15}N^\beta$ = 1.0417. Absolute relative difference (Eq. (31)) is the absolute value of the difference between the estimated value and actual value divided by the actual value (|(estimate – actual)/actual|). B. Comparison of the average RMSE values for each set of 1000 simulated datasets derived from Dataset 1. Both the standard Rayleigh model and the Expanded Rayleigh model (1 and 2) use $\delta^{15}N^{bulk}$ as the dependent variable, so average RMSE values can be compared directly. Lower RMSE values indicate a better goodness of fit. At each error level (low, medium, and high), the absolute relative difference value (A) or average RMSE (B) is depicted with a symbol that represents skewness type as shown in the legend. Note that in most cases these symbols overlap.

24

495 **Table 4. Precision and accuracy of values calculated with Expanded Rayleigh model 1 using simulated datasets derived from Dataset 1 (no isotope effect for N^α, normal isotope effect for N^β).**

Model	Level of error	Skewness	Standard Rayleigh $R^{2\ a,\ b}$	KIE $^{15}N^{bulk\ a}$	KIE $^{15}N^{\alpha\ a}$	KIE $^{15}N^{\beta\ a}$
Actual[c]	None	No	NA	$1.0204 \pm$ NA	$1 \pm$ NA	$1.0417 \pm$ NA
Expanded Rayleigh 1[d]	Low	No	0.95 ± 0.02	1.0202 ± 0.0013	0.9998 ± 0.0013	1.0414 ± 0.0014
		Left	0.94 ± 0.02	1.0202 ± 0.0013	0.9998 ± 0.0013	1.0414 ± 0.0014
		Right	0.94 ± 0.02	1.0202 ± 0.0013	0.9998 ± 0.0013	1.0415 ± 0.0014
Expanded Rayleigh 1[d]	Medium	No	0.75 ± 0.09	1.0196 ± 0.0031	0.9992 ± 0.0030	1.0408 ± 0.0032
		Left	0.74 ± 0.1	1.0197 ± 0.0032	0.9994 ± 0.0032	1.0409 ± 0.0033
		Right	0.74 ± 0.1	1.0197 ± 0.0031	0.9993 ± 0.0031	1.0410 ± 0.0033
Expanded Rayleigh 1[d]	High	No	0.44 ± 0.17	1.0186 ± 0.0060	0.9982 ± 0.0060	1.0398 ± 0.0061
		Left	0.43 ± 0.17	1.0190 ± 0.0058	0.9987 ± 0.0058	1.0401 ± 0.0061
		Right	0.43 ± 0.17	1.0187 ± 0.0059	0.9983 ± 0.0059	1.0400 ± 0.0062

[a] Average value $\pm$ standard deviation calculated from 1000 R^2 values generated from 1000 simulated datasets.

[b] Average R^2 value for linear regression of $\delta^{15}N^{bulk}$ against [-flnf/(1-f)] (using Eq. (2), the standard Rayleigh equation)
500 calculated from 1000 R^2 values generated from 1000 simulated datasets.

[c] Actual values were calculated directly from the input values used to generate the dataset.

[d] For Expanded Rayleigh model 1, α_{N-bulk} was determined with the standard Rayleigh approach, ρ was determined via nonlinear regression (nonlinear model 1, Eq. (29)), and τ was determined by averaging $^{14}N^\alpha/^{14}N^{bulk}$ for every step of the reaction (Eq. (24)). The results for Expanded Rayleigh model 2 (Table S9) are very similar.

505 **3.3 Application of the Expanded Rayleigh model to previously published isotopic data**

As a proof-of-concept example, we applied the standard Rayleigh model and the Expanded Rayleigh model to previously published experimental data and compared the results. We chose data collected for N_2O biosynthesis by a culture of *M. trichosporium* (*Methylocystis* sp.) grown aerobically in the presence of NH_2OH (Sutka et al., 2006). *Methylocystis* species encode the gene for hydroxylamine oxidoreductase (HAO), an enzyme that not only converts NH_2OH to NO during
510 nitrification, but also produces N_2O under certain conditions (Yamazaki et al., 2014). As *Methylocystis* species lack the gene for cytochrome P460 (which has also been shown to convert NH_2OH to N_2O) (Caranto et al., 2016), the isotopic fractionation observed in this experiment is assumed to be due to only one process: HAO-catalyzed conversion of NH_2OH to N_2O. Indeed, the ε_{N-bulk} value for N_2O produced in this experiment (5.3‰ $\pm$ 0.4 for replicate B (Table S15) (Sutka et al., 2006)) is very similar to the ε_{N-bulk} value of 2.0‰ reported for purified HAO from *Nitrosomonas europaea* (Yamazaki et al., 2014). The
515 differences between $\delta^{15}N^\alpha$ and $\delta^{15}N^\beta$ (SP) are also very similar for the two experiments, indicating that HAO was the primary source of N_2O production in the cultures of *M. trichosporium*, meaning the Rayleigh model could be applied to this system.

Application of the standard Rayleigh model (Eq. (2)) to $\delta^{15}N^{bulk}$ via linear regression of $\delta^{15}N^{bulk}$ against [-flnf/(1-f)] indicated that $\varepsilon_{N\text{-bulk}}$ was 5.3‰ ± 0.4 and KIE $^{15}N^{bulk}$ was 0.9947 ± 0.0004 (inverse isotope effect) (Table 5) for N_2O production by *M.trichosporium*. Similarly, application of the standard Rayleigh model to $\delta^{15}N^{\alpha}$ and $\delta^{15}N^{\beta}$ produced a KIE $^{15}N^{\alpha}$ value of

520 0.9952 ± 0.0015 and a KIE $^{15}N^{\beta}$ value of 0.9942 ± 0.0021. Thus, the standard Rayleigh model predicts an inverse isotope effect for both N^{α} and N^{β}, which theoretically means that both positions are enriched in ^{15}N relative to substrate. However, all of the $\delta^{15}N^{\beta}$ values (-11.7 to -13.3‰) are more negative than the measured $\delta^{15}N^{s0}$ value of -2.3‰ (Fig. 4 and Table S14), indicating that ^{15}N is *depleted* at the β position and that ^{14}N is preferred (normal isotope effect). The $\delta^{15}N^{\alpha}$ values (21.1 to 22.7‰), in contrast, are more positive than $\delta^{15}N^{s0}$, indicating that there is an inverse isotope effect at this position. The

525 Expanded Rayleigh model produces position-specific KIEs that match this qualitative assessment: KIE $^{15}N^{\alpha} = 0.9779 ± 0.0004$ (inverse), and KIE $^{15}N^{\beta} = 1.0121\text{-}1.0122 ± 0.0004$ (normal) (Table 5). Additionally, the values of ρ and τ do not vary significantly with f (Table S15), indicating that fractionation at the α and β positions appears to be constant. Comparison of the RMSE values for the standard (linear) Rayleigh model and the nonlinear portion of the Expanded Rayleigh model also indicates that both models have a similar goodness of fit. Thus, the Expanded Rayleigh model can be applied to experimental

530 data to accurately assess position-specific KIEs.

Table 5. Comparison of standard Rayleigh and Expanded Rayleigh KIE values ± standard error for N_2O produced from NH_2OH by an axenic culture of *M. trichosporium* (*Methylocystis* sp.). Values were calculated using isotopic data previously published for *M. trichosporium* replicate B (Sutka et al., 2006)].

Model	Standard Rayleigh (linear) RMSE [a]	Nonlinear RMSE [b]	KIE $^{15}N^{bulk}$ [c]	KIE $^{15}N^{\alpha}$ [c]	KIE $^{15}N^{\beta}$ [c]
Standard [d]	0.07	NA	0.9947 ± 4e-04	0.9952 ± 0.0015	0.9942 ± 0.0021
Expanded 1 [e]	0.07	0.16	0.9947 ± 4e-04	0.9779 ± 4e-04	1.0121 ± 4e-04
Expanded 2 [e]	0.07	0.16	0.9947 ± 4e-04	0.9779 ± 4e-04	1.0122 ± 4e-04

535

[a] RMSE (root mean square error) for standard Rayleigh model (Eq. (2), linear regression of $\delta^{15}N^{bulk}$ against [-flnf/(1-f)])

[b] RMSE for nonlinear model 1 or 2, Eq. (29) or Eq. (30)

[c] Average value ± standard error

[d] KIE values were calculated from $\varepsilon_{N\text{-bulk}}$, $\varepsilon_{N\text{-}\alpha}$, or $\varepsilon_{N\text{-}\beta}$ values obtained via linear regression of $\delta^{15}N^{bulk}$, $\delta^{15}N^{\alpha}$, or $\delta^{15}N^{\beta}$ against

540 [-flnf/(1-f)]).

[e] For the Expanded Rayleigh model, bulk values ($\alpha_{N\text{-bulk}}$, $\varepsilon_{N\text{-bulk}}$, and KIE $^{15}N^{bulk}$) were determined with the standard Rayleigh approach, ρ was determined via nonlinear regression (nonlinear model 1 or 2, Eq. (29) or Eq. (30)), and τ was determined by averaging $^{14}N^{\alpha}/^{14}N^{bulk}$ for every step of the reaction. Then $\alpha_{N\text{-}\alpha}$ and $\alpha_{N\text{-}\beta}$ were calculated with Eq. (21) or Eq. (22) and converted to KIE values using Eq. (10).

545

We also compared the results of applying the standard and Expanded Rayleigh models to previously published isotopic data on NO reduction to N_2O by purified *H. capsulatum* P450 NOR (Yang et al., 2014). In this experiment, $\delta^{15}N^{bulk}$ varied linearly with $[-flnf/(1-f)]$ ($R^2 = 0.68\text{-}0.94$), and averaging the slopes of the standard Rayleigh plots for each individual replicate indicated that $\varepsilon_{N\text{-bulk}}$ was equal to 9.10‰ ± 1.42 and KIE $^{15}N^{bulk}$ was equal to 0.9910 ± 0.0014 (Table 6 and Table S17). In other words, on average, N_2O became depleted in ^{15}N (*i.e.*, $\delta^{15}N^{bulk}$ decreased) as the reaction proceeded (Fig. 5 and Table S16). However, the N^α position became more enriched in ^{15}N as the reaction progressed (*i.e.*, $\delta^{15}N^\alpha$ increased as f decreased). Consequently, ρ increased (and τ decreased) over the course of the reaction (Table S17), and the observed values of $\alpha_{N\text{-}\alpha}$ and $\alpha_{N\text{-}\beta}$ also varied with f, in contrast to Assumption 6 (above). Thus, the Expanded Rayleigh model, which is based on the assumption that $\alpha_{N\text{-}\alpha}$ and $\alpha_{N\text{-}\beta}$ remain constant over the course of the reaction, does not fit this data optimally. Using a modified version of the Expanded Rayleigh model, however, we estimated apparent KIE $^{15}N^\alpha$ and KIE $^{15}N^\beta$ values for the beginning and end of the observed range of f values. Our estimated KIE $^{15}N^\alpha$ values ranged from 0.9823 ± 0.0016 (earlier in the reaction) to 0.9781 ± 0.0016 (later in the reaction), indicating that the N^α position is subject to an inverse isotope effect throughout the reaction. On the other hand, the KIE $^{15}N^\beta$ estimates ranged from 0.9998 ± 0.0015 to 1.0041 ± 0.0013, suggesting that there is essentially no apparent isotope effect at the β position, especially early in the reaction. These results are consistent with a qualitative assessment of the δ values. For example, the $\delta^{15}N^\alpha$ values (-25.8 to -31.0‰) are more positive than the calculated $\delta^{15}N^{s0}$ values (*i.e.*, the intercept of the standard Rayleigh plots for $\delta^{15}N^{bulk}$), which range from -44.7‰ to -48.3‰. This indicates that the α position is enriched in ^{15}N relative to the substrate. On the other hand, the $\delta^{15}N^\beta$ values near the start of the reaction (-45.2 to -48.3‰) are similar to the calculated $\delta^{15}N^{s0}$ values, suggesting that there is very little isotopic fractionation at the β position.

In contrast to the Expanded Rayleigh model estimates, the standard Rayleigh calculations yield a normal isotope effect for N^α (KIE $^{15}N^\alpha$ = 1.0127 ± 0.0030) and an inverse isotope effect for N^β (KIE $^{15}N^\beta$ = 0.9694 ± 0.002). While it is possible that N^β exhibits an apparent inverse isotope effect near the beginning of the reaction, the magnitude of this effect is likely much smaller (*i.e.*, early KIE $^{15}N^\beta$ is much closer to 1) than the standard Rayleigh calculations suggest. More strikingly, the standard Rayleigh prediction that N^α is subject to a normal isotope effect (^{14}N preferred) is clearly incorrect, as the α position is enriched in ^{15}N relative to the initial substrate. Moreover, as ^{15}N is depleted from the substrate pool, the fraction of ^{15}N incorporated into the α position *increases*, indicating that the preference for ^{15}N at N^α increases (becomes more inverse) as the reaction proceeds. Overall, analysis of the P450 NOR data demonstrates that even for reactions where the apparent position-specific KIEs vary, the Expanded Rayleigh model produces considerably more accurate KIE estimates than the standard Rayleigh model.

575

Table 6. Comparison of standard Rayleigh and Expanded Rayleigh KIE values ± standard error for N$_2$O production from NO by purified *Histoplasma capsulatum* (fungal) P450 NOR [calculated using previously published isotopic data (Yang et al., 2014)].

Model	Extent of reaction (range of f)		KIE ^{15}N^{bulk} [a]	KIE ^{15}N$^{\alpha}$ [a]	KIE ^{15}N$^{\beta}$ [a]
Standard [b]	All	0.42-0.87	0.9910 ± 0.0014	1.0127 ± 0.0030	0.9694 ± 0.0022
Expanded [c]	Early	0.77-0.81	0.9910 ± 0.0014	0.9823 ± 0.0016	0.9998 ± 0.0015
Expanded [c]	Late	0.47-0.52	0.9910 ± 0.0014	0.9781 ± 0.0016	1.0041 ± 0.0013

580

[a] Average value ± standard deviation calculated for values from three separate replicates (standard Rayleigh model KIEs and Expanded Rayleigh KIE ^{15}N^{bulk}) or for six (early) or seven (late) individual observations (Expanded Rayleigh model KIE ^{15}N$^{\alpha}$ and KIE ^{15}N$^{\beta}$). Individual early-reaction or late-reaction KIEs from all three replicates were pooled and averaged.

[b] KIE values were calculated from $\varepsilon_{N\text{-bulk}}$, $\varepsilon_{N\text{-}\alpha}$, or $\varepsilon_{N\text{-}\beta}$ values obtained via linear regression of δ^{15}N^{bulk}, δ^{15}N$^{\alpha}$, or δ^{15}N$^{\beta}$ against

585 [-flnf/(1-f)]). The standard Rayleigh model values presented here differ slightly from the previously published values (Yang et al., 2014) due to our exclusion of the earliest observation(s) from each replicate (*i.e.*, observations with the highest values of f were excluded).

[c] For the Expanded Rayleigh model, bulk values ($\alpha_{N\text{-bulk}}$, $\varepsilon_{N\text{-bulk}}$, and KIE ^{15}N^{bulk}) were determined with the standard Rayleigh approach. ρ was calculated for each observation using Eq. (23) ($\rho = {}^{15}$N$^{\alpha}/{}^{15}$N^{bulk}), and τ was determined for every step of the

590 reaction using Eq. (24) ($\tau = {}^{14}$N$^{\alpha}/{}^{14}$N^{bulk}). Then $\alpha_{N\text{-}\alpha}$ and $\alpha_{N\text{-}\beta}$ were calculated for each individual observation with Eq. (21) or Eq. (22) and converted to KIE values using Eq. (10).

4 Discussion

4.1 Proper application of the Expanded Rayleigh model

The Rayleigh model has been used to study kinetic isotope effects for decades and has been adapted many different times for

595 use in specific scenarios. However, to our knowledge, this is the first examination of how the Rayleigh model applies to a process where two heavy atoms from the same substrate pool (*e.g.*, NO or NH$_2$OH) are incorporated into non-equivalent positions in the product (*e.g.*, N$_2$O). Our simulations of different N$_2$O-producing scenarios demonstrate that the original Rayleigh model should not be applied to the individual atoms in such cases as this produces inaccurate results. However, the new Expanded Rayleigh model presented here can be used to accurately determine individual kinetic isotope effects. This

600 expanded model allows for a more granular analysis than would be possible from determining only bulk kinetic isotope effects and SP.

In practice, when can the Expanded Rayleigh model be used? To develop the Expanded Rayleigh model, we employed the same assumptions that the original model is founded on. Therefore, any situations where the original Rayleigh

model applies will also likely be suitable for the Expanded Rayleigh model. More specifically, the Expanded Rayleigh model

605   will likely produce accurate results for any closed system where N_2O is produced from a substrate pool with ^{15}N at or near natural abundance, *as long as the rate-determining step(s) for each atom remains constant*. Thus, the Expanded Rayleigh model is ideally suited for studies of isolated N_2O-synthesizing enzymes, as this experimental setup provides a closed system where N_2O is produced by a single catalytic process.

One method for confirming that the rate-determining steps of N_2O synthesis are constant is to determine if $\varepsilon_{N\text{-bulk}}$ and

610   SP are constant for a particular dataset. If enzymatic catalysis is rate-limiting throughout a time course experiment, $\varepsilon_{N\text{-bulk}}$ will be constant, and the slope of a standard Rayleigh plot should be linear. In contrast, if substrate diffusion (or some other process) becomes rate-limiting, curvilinear behavior may be exhibited in a standard Rayleigh plot, as has been observed for multi-step N_2O production in microbial cultures (Sutka et al., 2008; Haslun et al., 2018). Of course, to use the Expanded Rayleigh model, $\varepsilon_{N\text{-}\alpha}$ and $\varepsilon_{N\text{-}\beta}$ must be constant as well. To verify that the individual fractionation factors are constant, one could plot $\delta^{15}N^\alpha$ and

615   $\delta^{15}N^\beta$ against $[-f\ln f/(1-f)]$ (*i.e.*, create standard Rayleigh plots for $\delta^{15}N^\alpha$ and $\delta^{15}N^\beta$) and confirm that these plots are linear and roughly parallel. Alternatively, SP (the difference of $\delta^{15}N^\alpha$ and $\delta^{15}N^\beta$, Eq. (32)) can be monitored over time. A lack of a significant trend in SP values is a reasonably good indication that $\varepsilon_{N\text{-}\alpha}$ and $\varepsilon_{N\text{-}\beta}$ are constant. In studies of microbial cultures where N_2O is predominantly produced by a single type of enzyme (*e.g.*, bacterial NOR, fungal NOR, or HAO), SP generally remains constant as substrate is consumed (Toyoda et al., 2005; Sutka et al., 2006; Sutka et al., 2008; Haslun et al., 2018). The

620   fact that SP is constant for a variety of N_2O production pathways in a microbial cell suggests that enzyme-specific fractionation at N^α and N^β typically remains constant, meaning the Expanded Rayleigh model can likely be accurately applied to a variety of N_2O-producing enzymes.

At present, there is a scarcity of studies reporting N_2O fractionation by purified enzymes for multiple values of f, limiting our ability to test the Expanded Rayleigh model with published experimentally-derived datasets. We were, however,

625   able to apply the Expanded Rayleigh model to previously published data on *M. trichosporium* cultures (Sutka et al., 2006), whose HAO-catalyzed oxidation of NH_2OH was the primary source of N_2O and displayed constant values of $\varepsilon_{N\text{-bulk}}$ and SP. Thus, we were able to calculate observed values of KIE $^{15}N^\alpha$ and KIE $^{15}N^\beta$ that serve as reasonable estimates of HAO-specific isotope effects (Table 5). Additionally, we have used the Expanded Rayleigh model to re-evaluate isotopic data our group has collected for purified fungal P450 NOR (Table 6) (Yang et al., 2014). The value of $\varepsilon_{N\text{-bulk}}$ for P450 NOR appears to be constant,

630   but SP increased by 14‰ as the fraction of NO reduced changed from 10% to 50% (Yang et al., 2014). Given the proposed P450 NOR reaction mechanism, the observed isotope effect for the first NO molecule is influenced both by an equilibrium isotope effect related to NO binding and by an intrinsic KIE associated with catalysis (Yang et al., 2014). Conversely, the rate-determining step(s) for the second NO molecule are likely only associated with catalysis. Thus, the isotopic fractionation for the first nitrogen atom to be incorporated will be more sensitive to changes in NO concentration as the reaction progresses

635   than the second N atom, leading to SP values that are not constant. Even in these circumstances, however, the Expanded Rayleigh model estimates for KIE $^{15}N^\alpha$ and KIE $^{15}N^\beta$ are a significant improvement on the previously published standard

Rayleigh estimates, which incorrectly predict a normal isotope effect at the α position. Overall, the Expanded Rayleigh model fits the available data on isotopic fractionation during N_2O biosynthesis reasonably well, although we recommend collecting isotopic data across a range of f values to confirm that SP (and therefore KIE $^{15}N^{\alpha}$ and KIE $^{15}N^{\beta}$) remains constant when using

640   this model.

As outlined above ("Assumptions"), the Expanded Rayleigh model is most accurate for reactions where the isotopic fractionation factors (ε_{N-bulk}, $\varepsilon_{N-\alpha}$, and $\varepsilon_{N-\beta}$) and $\delta^{15}N^{s0}$ values are not too extreme. This stipulation, which also applies to the standard Rayleigh equation, is necessary in part because an approximation introduced by Mariotti and colleagues (Mariotti et al., 1981) decreases in accuracy the farther $\delta^{15}N^{s0}$ and $\delta^{15}N^{s}$ are from 0‰. Additionally, extremely high, positive values of

645    $\delta^{15}N^{s0}$ or ε_{N-bulk} would result in large, positive product δ values, corresponding to an increased abundance of ^{15}N in the product. As both the nonlinear Rayleigh model and the underlying calculation of $\delta^{15}N^{\beta}$ values depend on the assumption that the amount of ^{15}N in N_2O is close to natural abundance, the accuracy of the Expanded Rayleigh model would decrease in such circumstances. Thus, applying the Expanded Rayleigh model to experiments with spiked ^{15}N is not advised. Simulations of δ values calculated without using Mariotti's approximation indicate that for absolute values of ε_{N-bulk} or $\delta^{15}N^{s0}$ less than or equal

650   to 50‰, the level of error introduced by Mariotti's approximation is similar to the expected level of experimental error (*i.e.*, absolute relative difference in KIE values of ~0.001) (Tables S1-S2).

The magnitude of $\varepsilon_{N-\alpha}$ and $\varepsilon_{N-\beta}$ must also be considered when applying the Expanded Rayleigh model. In theory, if isotopic enrichment at N^{α} or N^{β} is very large, the assumption that essentially equal amounts of ^{14}N are apportioned to each position (*i.e.*, that $\tau \approx 0.5$) would be violated, and Eq. (15) would no longer hold. However, violating this assumption would

655   require unusually large heavy-atom kinetic isotope effects or a spiked sample. As outlined in Table S3, for a simulated reaction where ε_{N-bulk} is set at -20‰ and $\delta^{15}N^{s0}$ is 0‰ (KIE $^{15}N^{bulk} = 1.0204$), individual KIE values would have to be significantly lower than 0.96 or greater than 1.08 to introduce error greater than analytical error. These KIE $^{15}N^{\alpha}$ or KIE $^{15}N^{\beta}$ values correspond to ρ values less than 0.47 or greater than 0.53. In practice, our group has found that for two different types of N_2O-producing enzymes, ρ is nowhere near these extremes. For example, for purified P450 NOR (Yang et al., 2014) and for HAO-

660   catalyzed NH_2OH oxidation in an axenic culture (Sutka et al., 2006), ρ does not exceed 0.509 (Table S15, Table S17). Overall, we anticipate that the Expanded Rayleigh model will be applicable to a wide variety of N_2O biosynthesis reactions.

4.2 Other practical considerations

The Expanded Rayleigh model presented here does not require measurement of $\delta^{15}N^{s0}$. This is advantageous for N_2O synthesis reactions where NO is the substrate because directly measuring an accurate $\delta^{15}N$ value for NO is quite challenging

665   due to the reactivity of NO, the lack of isotopic standards for NO, and the fact that $^{14}N^{16}O$ has the same molecular weight as $^{15}N^{15}N$. However, $\delta^{15}N^{s0}$ can be directly measured when NH_2OH is used as the substrate for N_2O production. Determining $\delta^{15}N^{s0}$ experimentally may be useful in validating application of the standard Rayleigh model, as the intercept of the standard Rayleigh model is expected to be equal to $\delta^{15}N^{s0}$. For example, we determined that the intercept of the standard Rayleigh plot

for N$_2$O produced by NH$_2$OH oxidation by *M. trichosporium* is 0.5 ± 0.3‰, which is similar to the measured δ^{15}N^{s0} value of

670 -2.3‰ (Sutka et al., 2006), confirming that the standard Rayleigh model is applicable for this dataset. Thus, when feasible, measuring δ^{15}N^{s0} would complement the Expanded Rayleigh approach.

The nonlinear portion of the Expanded Rayleigh model (used to determine ρ) can be written in two forms, nonlinear model 1 (Eq. (29)) and nonlinear model 2 (Eq. (30)). Both models are based on the assumption that δ^{15}N^{bulk} is equal to the average of δ^{15}N^{α} and δ^{15}N^{β} (Eq. (15)). Therefore, both models are expected to produce very similar results as long as that

675 assumption holds. Indeed, as we have demonstrated here, both models yield nearly identical values of ρ, KIE ^{15}N^{α}, and KIE ^{15}N^{β} for simulated datasets (Fig. 6, Figs. S5-S8, Tables S9-S13), and we have obtained similar results for the available experimental data on N$_2$O production from NH$_2$OH (Table 5). Thus, either version of the Expanded Rayleigh model may be used. If there is any doubt about which version to use, we recommend selecting the model that has a lower RMSE value (and thus fits the data better).

680 **5 Conclusions**

In this manuscript, we presented the Expanded Rayleigh model, a novel adaptation of the Rayleigh distillation equation that describes the position-specific isotopic enrichment that occurs at N^{α} and N^{β} during N$_2$O synthesis. Using simulated datasets representing multiple different combinations of KIEs, we demonstrated that the Expanded Rayleigh model accurately recapitulates KIE ^{15}N^{α} and KIE ^{15}N^{β} for a wide variety of scenarios. Our simulations also demonstrate that this new

685 model is robust even when applied to skewed data and/or data with a high level of error. Additionally, we have shown the Expanded Rayleigh model fits the experimentally-measured isotopic data for N$_2$O production from NH$_2$OH quite well (Sutka et al., 2006) and provides significantly improved estimates for the position-specific KIEs for P450 NOR-catalyzed N$_2$O synthesis. Thus, the Expanded Rayleigh model provides a reliable method for quantifying isotopic fractionation at N^{α} and N^{β}, and it promises to be a valuable tool for experimentally probing the catalytic mechanisms of N$_2$O-synthesizing enzymes.

690 Finally, we note that the Expanded Rayleigh model will also likely be appropriate for the analysis of other reactions where two atoms from the same substrate pool are incorporated into distinct, non-exchangeable positions in the product.

Code and data availability

All code used in this manuscript is available at:
https://github.com/GLBRC/position-specific-KIE

695

The results for each of the 1000 simulations with error (derived from Datasets 1-5) can be found at:
https://zenodo.org/records/10888931

Author contribution

EDR, NEO, and ELH conceived this study. EDR developed the model and analyzed the data with contributions from WM,
700   NEO, and ELH. WM provided critical input for statistical analysis and coding. EDR prepared the original draft of the
manuscript and figures, and all authors participated in editing and revision of the manuscript.

Competing interests

The authors declare that they have no conflict of interest.

Acknowledgements

References

Azzalini, A.: The R package 'sn': The Skew-Normal and Related Distributions such as the Skew-t and the SUN (version 2.1.1).
715   URL http://azzalini.stat.unipd.it/SN/,https://cran.r-project.org/package=sn [code], 2023.

Baty, F., Ritz, C., Charles, S., Brutsche, M., Flandrois, J.-P., and Delignette-Muller, M.-L.: A Toolbox for Nonlinear
        Regression in R: The Package nlstools, J Stat Softw, 66, 1 - 21, 10.18637/jss.v066.i05, 2015.

Bigeleisen, J. and Wolfsberg, M.: Theoretical and experimental aspects of isotope effects in chemical kinetics, Adv Chem
        Phys, 1, 15-76, 1958.

720   Caranto, J. D., Vilbert, A. C., and Lancaster, K. M.: *Nitrosomonas europaea* cytochrome P460 is a direct link between
        nitrification and nitrous oxide emission, PNAS, 113, 14704-14709, 10.1073/pnas.1611051113, 2016.

Frame, C. H. and Casciotti, K. L.: Biogeochemical controls and isotopic signatures of nitrous oxide production by a marine
        ammonia-oxidizing bacterium, Biogeosciences, 7, 2695-2709, 10.5194/bg-7-2695-2010, 2010.

Haslun, J. A., Ostrom, N. E., Hegg, E. L., and Ostrom, P. H.: Estimation of isotope variation of N_2O during denitrification by
725   *Pseudomonas aureofaciens* and *Pseudomonas chlororaphis*: implications for N_2O source apportionment,
         Biogeosciences, 15, 3873-3882, 10.5194/bg-15-3873-2018, 2018.

Hippel, P. v.: Skewness, in: International Encyclopedia of Statistical Science, edited by: Lovric, M., Springer Berlin
         Heidelberg, Berlin, Heidelberg, 1340-1342, 10.1007/978-3-642-04898-2_525, 2011.

Junk, G. A. and Svec, H. J.: Nitrogen isotope abundance measurements, US atomic energy commission. Office of technical
730   information., ISC 1138, 1958.

Kalpić, D., Hlupić, N., and Lovrić, M.: Student's t-Tests, in: International Encyclopedia of Statistical Science, edited by:
         Lovric, M., Springer Berlin Heidelberg, Berlin, Heidelberg, 1559-1563, 10.1007/978-3-642-04898-2_641, 2011.

Komsta, L. and Novomestky, F.: moments: Moments, Cumulants, Skewness, Kurtosis and Related Tests. R package version
         0.14.1, https://CRAN.R-project.org/package=moments. [code], 2022.

735 Kuypers, M. M. M., Marchant, H. K., and Kartal, B.: The microbial nitrogen-cycling network, Nat Rev Microbiol, 16, 263-
         276, 10.1038/nrmicro.2018.9, 2018.

Trends in globally-averaged CH_4, N_2O, and SF_6 determined from NOAA Global Monitoring Laboratory measurements.
         Version 2023-11, last access: 11/27/2023.

Lehnert, N., Dong, H. T., Harland, J. B., Hunt, A. P., and White, C. J.: Reversing nitrogen fixation, Nat Rev Chem, 2, 278-
740   289, 10.1038/s41570-018-0041-7, 2018.

Mariotti, A., Germon, J. C., Hubert, P., Kaiser, P., Letolle, R., Tardieux, A., and Tardieux, P.: Experimental determination of
         nitrogen kinetic isotope fractionation: Some principles; illustration for the denitrification and nitrification processes,
         Plant Soil, 62, 413-430, 10.1007/BF02374138, 1981.

R Core Team: R: A language and environment for statistical computing, R
745   Foundation for Statistical Computing, Vienna, Austria,
      https://www.R-project.org/. [code], 2022.

Ravishankara, A. R., Daniel, J. S., and Portmann, R. W.: Nitrous oxide (N_2O): The dominant ozone-depleting substance
         emitted in the 21st century, Science, 326, 123-125, doi:10.1126/science.1176985, 2009.

Ritz, C. and Streibig, J. C.: Nonlinear Regression with R. [electronic resource], 1st ed. 2008., Use R!, Springer New York2008.

750 Romão, C. V., Vicente, J. B., Borges, P. T., Frazão, C., and Teixeira, M.: The dual function of flavodiiron proteins: oxygen
         and/or nitric oxide reductases, J Biol Inorg Chem, 21, 39-52, 10.1007/s00775-015-1329-4, 2016.

Scott, K. M., Lu, X., Cavanaugh, C. M., and Liu, J. S.: Optimal methods for estimating kinetic isotope effects from different
         forms of the Rayleigh distillation equation, Geochim Cosmochim Ac, 68, 433-442, 10.1016/s0016-7037(03)00459-
         9, 2004.

755 Stocker, T. F., D. Qin, G.-K. Plattner, M. Tignor, S.K. Allen, J. Boschung, A. Nauels, Y. Xia, V. Bex and P.M. Midgley,
         Press, C. U. (Ed.): IPCC, 2013: Climate Change 2013: The Physical Science Basis. Contribution of Working Group

I to the Fifth Assessment Report of the Intergovernmental Panel on Climate Change, Cambridge, United Kingdom and New York, NY, USA2013.

summary.lm: Summarizing Linear Model Fits. R package stats (version 3.6.2):
760 https://www.rdocumentation.org/packages/stats/versions/3.6.2/topics/summary.lm, last access: 12/12/2023.

Sutka, R. L., Adams, G. C., Ostrom, N. E., and Ostrom, P. H.: Isotopologue fractionation during N_2O production by fungal denitrification, Rapid Commun Mass Sp, 22, 3989-3996, 10.1002/rcm.3820, 2008.

Sutka, R. L., Ostrom, N. E., Ostrom, P. H., Gandhi, H., and Breznak, J. A.: Nitrogen isotopomer site preference of N_2O produced by *Nitrosomonas europaea* and *Methylococcus capsulatus* Bath, Rapid Commun Mass Sp, 17, 738-745,
765 10.1002/rcm.968, 2003.

Sutka, R. L., Ostrom, N. E., Ostrom, P. H., Gandhi, H., and Breznak, J. A.: Nitrogen isotopomer site preference of N_2O produced by *Nitrosomonas europaea* and *Methylococcus capsulatus* Bath, Rapid Commun Mass Sp, 18, 1411-1412, https://doi.org/10.1002/rcm.1482, 2004.

Sutka, R. L., Ostrom, N. E., Ostrom, P. H., Breznak, J. A., Gandhi, H., Pitt, A. J., and Li, F.: Distinguishing nitrous oxide
770 production from nitrification and denitrification on the basis of isotopomer abundances, Appl Environ Microb, 72, 638-644, 10.1128/aem.72.1.638-644.2006, 2006.

Tian, H., Xu, R., Canadell, J. G., Thompson, R. L., Winiwarter, W., Suntharalingam, P., Davidson, E. A., Ciais, P., Jackson, R. B., Janssens-Maenhout, G., Prather, M. J., Regnier, P., Pan, N., Pan, S., Peters, G. P., Shi, H., Tubiello, F. N., Zaehle, S., Zhou, F., Arneth, A., Battaglia, G., Berthet, S., Bopp, L., Bouwman, A. F., Buitenhuis, E. T., Chang, J.,
775 Chipperfield, M. P., Dangal, S. R. S., Dlugokencky, E., Elkins, J. W., Eyre, B. D., Fu, B., Hall, B., Ito, A., Joos, F., Krummel, P. B., Landolfi, A., Laruelle, G. G., Lauerwald, R., Li, W., Lienert, S., Maavara, T., MacLeod, M., Millet, D. B., Olin, S., Patra, P. K., Prinn, R. G., Raymond, P. A., Ruiz, D. J., van der Werf, G. R., Vuichard, N., Wang, J., Weiss, R. F., Wells, K. C., Wilson, C., Yang, J., and Yao, Y.: A comprehensive quantification of global nitrous oxide sources and sinks, Nature, 586, 248-256, 10.1038/s41586-020-2780-0, 2020.

780 Toyoda, S. and Yoshida, N.: Determination of nitrogen isotopomers of nitrous oxide on a modified isotope ratio mass spectrometer, Anal Chem, 71, 4711-4718, 10.1021/ac9904563, 1999.

Toyoda, S., Mutobe, H., Yamagishi, H., Yoshida, N., and Tanji, Y.: Fractionation of N_2O isotopomers during production by denitrifier, Soil Biol Biochem, 37, 1535-1545, https://doi.org/10.1016/j.soilbio.2005.01.009, 2005.

Wickham, H.: ggplot2: Elegant Graphics for Data Analysis, Springer-Verlag New York. [code], 2016.

785 Yamazaki, T., Hozuki, T., Arai, K., Toyoda, S., Koba, K., Fujiwara, T., and Yoshida, N.: Isotopomeric characterization of nitrous oxide produced by reaction of enzymes extracted from nitrifying and denitrifying bacteria, Biogeosciences, 11, 2679-2689, 10.5194/bg-11-2679-2014, 2014.

Yang, H., Gandhi, H., Ostrom, N. E., and Hegg, E. L.: Isotopic fractionation by a fungal P450 nitric oxide reductase during the production of N_2O, Environ Sci Technol, 48, 10707-10715, 10.1021/es501912d, 2014.